Graduate School ETD Form 9
(Revised 12/07)

PURDUE UNIVERSITY
GRADUATE SCHOOL
Thesis/Dissertation Acceptance

This is to certify that the thesis/dissertation prepared

By Alejandro Galvis

Entitled
ADVANCING PROFILING SENSORS WITH A WIRELESS APPROACH

For the degree of Master of Science in Electrical and Computer Engineering

Is approved by the final examining committee:

David J. Russomanno
Chair

Feng Li

Maher Rizkalla

To the best of my knowledge and as understood by the student in the *Research Integrity and Copyright Disclaimer (Graduate School Form 20)*, this thesis/dissertation adheres to the provisions of Purdue University's "Policy on Integrity in Research" and the use of copyrighted material.

Approved by Major Professor(s): David J. Russomanno

Approved by: Brian King 11/20/2012
Head of the Graduate Program Date

Graduate School Form 20
(Revised 9/10)

PURDUE UNIVERSITY
GRADUATE SCHOOL

Research Integrity and Copyright Disclaimer

Title of Thesis/Dissertation:
ADVANCING PROFILING SENSORS WITH A WIRELESS APPROACH

For the degree of Master of Science in Electrical and Computer Engineering

I certify that in the preparation of this thesis, I have observed the provisions of *Purdue University Executive Memorandum No. C-22*, September 6, 1991, *Policy on Integrity in Research.**

Further, I certify that this work is free of plagiarism and all materials appearing in this thesis/dissertation have been properly quoted and attributed.

I certify that all copyrighted material incorporated into this thesis/dissertation is in compliance with the United States' copyright law and that I have received written permission from the copyright owners for my use of their work, which is beyond the scope of the law. I agree to indemnify and save harmless Purdue University from any and all claims that may be asserted or that may arise from any copyright violation.

Alejandro Galvis
Printed Name and Signature of Candidate

11/16/2012
Date (month/day/year)

*Located at http://www.purdue.edu/policies/pages/teach_res_outreach/c_22.html

ADVANCING PROFILING SENSORS

WITH A WIRELESS APPROACH

A Thesis

Submitted to the Faculty

of

Purdue University

by

Alejandro Galvis

In Partial Fulfillment of the

Requirements for the Degree

of

Master of Science in Electrical and Computer Engineering

December 2012

Purdue University

Indianapolis, Indiana

ACKNOWLEDGMENTS

Funding for this work was provided in part by the US Army Research Laboratory (ARL) award number: W911NF-10-2-0071, as well as support from Indiana University-Purdue University Indianapolis and the University of Memphis. The findings and opinions expressed in this thesis do not necessarily reflect the views of ARL or the US government.

TABLE OF CONTENTS

Page

LIST OF TABLES

LIST OF FIGURES

Figure Page

Figure Page

LIST OF SYMBOLS

α	Projection angle below the cone's height line.
β	Projection angle above the cone's height line.
ϕ	Internal cone base angle.
Δt	Recorded event time length.
c	Number columns in the compressed matrix.
d	Size of sliding window.
n	Number columns in the original matrix.
r	Remainder.
FOV_m	Minimum field of view.
h_c	Cone height.
M	Number of sensing elements in the array.
P_1	Input port 1.
P_2	Input port 2.
r_b	Cone base radius.
s_i	Sensing element in the i^{th} position.
t_0	Time in ms of first packet received in Δt.
t_a	Starting time in ms of a constant state interval within Δt.
t_b	Ending time in ms of a constant state interval within Δt.
t_f	Time in ms of last packet received in Δt.
v_{ih}	Weight values from the input to the hidden layer.
v_{ij}	Velocity among sensing elements i and j.
w_{ji}	Weight values from the hidden to the output layer.

LIST OF ABBREVIATIONS

ABS	Acrylonitrile Butadiene Styrene.
ARL	US Army Research Laboratory.
DB-37	Data Bus-37.
CAT6	Category 6.
DHS	Department of Homeland Security.
FOV	Field of View.
I/O	Input/Output.
IDC	Insulation-Displacement Connector.
IR	Infrared.
LCD	Liquid Crystal Display.
LWIR	Long Wave Infrared.
MTI	Moving Target Indication.
N-IR	Near-Infrared.
NiMH	Nickel-Metal Hydride.
NPN	Positive Negative Positive.
OEM	Original Equipment Manufacturer.
PC	Personal Computer.
PVC	Polyvinyl Chloride.
RF	Radio Frequency.
RJ-45	Registered Jack-45.
RS-232	Recommended Standard-232.
SBI.net	Secure Border Initiative .net.
US	United States.

USB	Universal Serial Bus.
USB-DIO-32	Universal Serial Bus-Digital Input/Output-32.

ABSTRACT

Galvis, Alejandro. M.S.E.C.E., Purdue University, December 2012. Advancing Profiling Sensors with a Wireless Approach. Major Professor: David J. Russomanno.

In general, profiling sensors are low-cost crude imagers that typically utilize a sparse detector array, whereas traditional cameras employ a dense focal-plane array. Profiling sensors are of particular interest in applications that require classification of a sensed object into broad categories, such as human, animal, or vehicle. However, profiling sensors have many other applications in which reliable classification of a crude silhouette or profile produced by the sensor is of value. The notion of a profiling sensor was first realized by a Near-Infrared (N-IR), retro-reflective prototype consisting of a vertical column of sparse detectors. Alternative arrangements of detectors have been implemented in which a subset of the detectors have been offset from the vertical column and placed at arbitrary locations along the anticipated path of the objects of interest. All prior work with the N-IR, retro-reflective profiling sensors has consisted of wired detectors. This thesis surveys prior work and advances this work with a wireless profiling sensor prototype in which each detector is a wireless sensor node and the aggregation of these nodes comprises a profiling sensor's field of view. In this novel approach, a base station pre-processes the data collected from the sensor nodes, including data re-alignment, prior to its classification through a back-propagation neural network. Such a wireless detector configuration advances deployment options for N-IR, retro-reflective profiling sensors.

1. INTRODUCTION

A sensor with a sparse detector array is a crude imaging device when compared to state-of-the-art imagers. High-end imaging devices utilize dense focal-plane arrays often producing images of high fidelity for subsequent object classification. Profiling sensors must be easily deployable on a large scale and are often regarded as disposable devices in applications that require surveillance of large, remote areas, which are often in hostile environments. Because of the relatively sparse number of sensing elements, these sensors are less expensive and produce a two-dimensional profile or silhouette of zero-dimensional samples. Profiling sensors are ideal for applications that require object classification using inexpensive, unmanned surveillance networks because of their low-cost components and efficient classification algorithms [1].

One such application of this technology that has garnered increased attention is intelligent fence applications [2], including security and surveillance of the United States (US) and other areas. The US has approximately $12,000$ kilometers of border, with numerous isolated and unpopulated sections. To improve the security of these borders by reducing smuggling and other illegal activities, improved surveillance is a top priority.

An approach to neutralizing crime in such a large areas has been the research and development of low-cost profiling sensors that can reliably discriminate among humans, animals, and vehicles. Profiling sensors can be used as surveillance devices to monitor trails and small unguarded roads, for example, border areas between the US and Mexico that are used for illegal trafficking and smuggling of contraband. Reliably classifying objects that traverse these routes is of high interest in defense and homeland security applications [1, 3–5].

Currently, it is not economically feasible to monitor an area as extensive as the US and Mexico border due to the cost and maintenance associated with traditional,

high-cost imagers and other sensing devices. The Department of Homeland Security (DHS), through the Secure Border Initiative .net (SBI.net) project, is the pioneer in the development of major border security devices for highly trafficked areas [6]. Infrared cameras and moving target indication (MTI) are examples of advanced sensing equipment that can operate in a network-centric environment to track human activity across a boarder. However, when completed, the deployment of such equipment along the US boarder is estimated to be $620K per km (approximately $1 million dollars per mile of border) [7]. With the exorbitant expense for full surveillance coverage using the SBI.net project system, the low-cost alternative of a profiling sensor network is of interest, either as a complementary or competing technology.

The concept of a sparse detector array profiling sensor, first proposed by R. Sartain from the US Army Research Laboratory, utilizes a crude image (silhouette or profile) produced by the sparse detector array to classify passing objects as a means of surveillance in remote locations [8]. A vertical detector array, consisting of sixteen pairs of transmitters and reflectors, was first developed to produce sixteen parallel N-IR beams. A silhouette was then generated if the object broke the sensor's beams [8–12]. Although a sparse detector array is less expensive to implement, it can be harder to conceal. Whereas traditional cameras, including infrared imaging sensors, require a dense focal-plane array to capture the entirety of a given field of view (FOV), a profiling sensor uses a sparse detector array to cover limited sampled sections of a FOV [2]. The reduced data sensed from the FOV limits the types of conclusions that can be drawn about the sensed objects, nevertheless, the types of conclusions that can be reliably deduced may satisfy the majority of the requirements of intelligent fence and analogous applications.

This thesis extends prior work in profiling sensors. The sensor presented in this thesis incorporates a wireless sensing element, a distributed data collection and aggregation scheme, an enhanced classification technique, as well as other hardware improvements to advance profiling sensors. These enhancements improve deployment

options as compared to the first generation of wired profiling sensors [13], possibly increasing the application scenarios for such sensors.

This thesis includes a review of representative work in wired profiling sensors. The foundational research of these previous wired profiling sensors led towards designing and building a novel wireless hardware prototype, which includes new contributions in data collection, processing, and classification. The major contributions of this thesis have been published in parallel to this thesis by Galvis et al. [14, 15]. This thesis augments and subsumes those publications and provides a broader context for the author's work. Chapter 2 presents the assembly, data acquisition, and associated software of the wired and wireless profiling sensors. However, the work in wired profiling sensors presented in Chapter 2.1 is purely given as background work to give context to the novel wireless profiling sensor prototype discussed in Chapter 3. Likewise, Chapter 4 highlights some alternative approaches to realizing profiling sensors, but these are not included as the novel contributions by the author of this thesis; these alternative approaches to profiling sensors are merely provided as a reference of complementary but distinct work. Lastly, Chapter 5 provides conclusions and recommendations for future work.

2. WIRED PROFILING SENSORS THAT USE A SPARSE DETECTOR ARRAY

The majority of the research in profiling sensors uses sparse detector arrays to create crude images via a sparse binary matrix that is converted into a silhouette. Using additional software and classification algorithms, these silhouettes can be identified as belonging to one of several predefined object classifications. In this chapter, we highlight the advances made in the wired profiling sensor iterations that lead to a novel wireless profiling sensor design. The wired iterations developed by previous researchers provides the foundational research to the wireless profiling sensor approach, which is the newest contribution in the family N-IR profiling sensors that use a sparse detector array. Furthermore, to highlight the latest work completed with N-IR profiling sensors, three major new contributions of the wireless profiling sensor are discussed in detail along with the challenges this new prototype presents.

One highly appropriate application for a device such as a profiling sensor is for the surveillance and monitoring of the US border. With this system, a passing object can be classified to determine if a manned response is necessary. Currently, the remote areas of the border are often monitored with vibration sensors that are unable to distinguish the type of nearby object but standardly result in a manned response to the area [16]. Implementing the profiling sensor system has the potential to reduce the number of unnecessary manned responses compared to the current vibration sensor system deployed in remote areas. Furthermore, through object classification, the manned response would be alerted to the severity of the breach and be able to respond accordingly. Thus, increasing the safety and efficiency of the manned responses along the border.

The original sparse detector N-IR profiling sensor prototypes were built using a collection of sixteen pairs of transmitters and reflectors to produce sixteen parallel

N-IR beams. The first prototype model of the profiling sensor consisted of a vertical arrangement of these transmitters and receivers. The transmitters are mounted on the first pole and create a N-IR beam that is perpendicular to the paired reflecting surface mounted on the opposite pole. In this configuration, the vertical profiling sensor has repeatedly shown to successfully generate and accurately classify silhouette images among defined classification groups when surveilling a specified trail [8–12]. For the initial prototype, there is zero horizontal offset between the transmitters and receivers. In laboratory practice, this reduces the amount of processing necessary to generate a crude silhouette since no further realignment algorithms are needed before classification can occur. However, having a vertical profiling sensor was deemed impractical in field testings due to concealment difficulties. Since the intended deployment region is along the US-Mexican border in the desertic Southwestern United States, the only natural camouflage is low lying shrubbery and cacti. Using the limitations of the natural camouflage in this region as the design criteria, a second iteration of profiling sensor was developed.

Ideally, these profiling sensors would be dusted along the US border using sporadic deployment to ensure full and randomized coverage over this region. The improvements in the second prototype work towards this goal by primarily focusing on the concealment and off-line data collection of the device. This prototype iteration uses the same sensing elements, transmitter, and reflecting surface as the vertical prototype but in an configuration with horizontal offsets between sensing elements [17,18]. Additional hardware improvements were made to eliminate the need of a computer in the field. An embedded microcontroller, Digi International BL4S200 single-board-computer, is used to prove that collecting, storing, realigning, and classifying data could be performed by a low resource device. In addition, a hand-held interface I/O box, made in-house at the University of Memphis, facilitates data access through the microcontroller to view classification results in the field.

The vertical and the custom array profiling sensor models proved that objects can be classified by examining their silhouettes and that data collection, realignment, and

classification operations can be successfully performed by a low resource device [17,18]. However, to reach the ideal deployment and operational state as described above, the profiling sensor must function wirelessly. Since these two prototypes do not possess the much needed wireless feature, a third prototype was developed, focusing largely on the conversion of the wired customizable profiling sensor prototype to a sustainable wireless model for remote deployment [14].

The following subchapters will provide a more detailed overview regarding hardware, assembly, and data capture of the wired profiling sensors. Chapter 2.1.1 will describe the most relevant specifications of the SUNX CX-RVM5 sensing element used in both wired profiling sensors. Chapter 2.1.2, will briefly show how the assembly of vertical and custom array profiling sensors was performed. Finally, Chapter 2.1.3 discusses methods of data acquisition and realignment used in wired profiling sensors.

2.1 Wired Vertical And Custom Array Profiling Sensors

The original sparse detector N-IR profiling sensor prototypes were built by previous researchers using a collection of sixteen pairs of transmitters and reflectors to produce sixteen parallel N-IR beams. The first prototype of the profiling sensor consisted of a vertical arrangement of these transmitters and receivers mounted on a platform with two separate poles. The transmitters were mounted on the first pole and create a N-IR beam that is perpendicular to the paired reflecting surface mounted on the opposite pole (Figure 2.1(a)). In this configuration, the vertical profiling sensor has been shown to successfully generate and accurately classify silhouettes among predefined classification groups [8–12]. For this initial prototype, there was a zero horizontal offset between the transmitters and receivers. In laboratory practice, this arrangement of transmitters and receivers reduces the amount of processing necessary to generate a crude silhouette since no further realignment algorithms are needed before classification algorithms are executed. However, a vertical array of detectors with

no horizontal offset induces deployment constraints that limit applications in several instances. A second iteration of profiling sensor was developed with the capability to horizontally offset the detectors, providing additional deployment flexibility for such sensors.

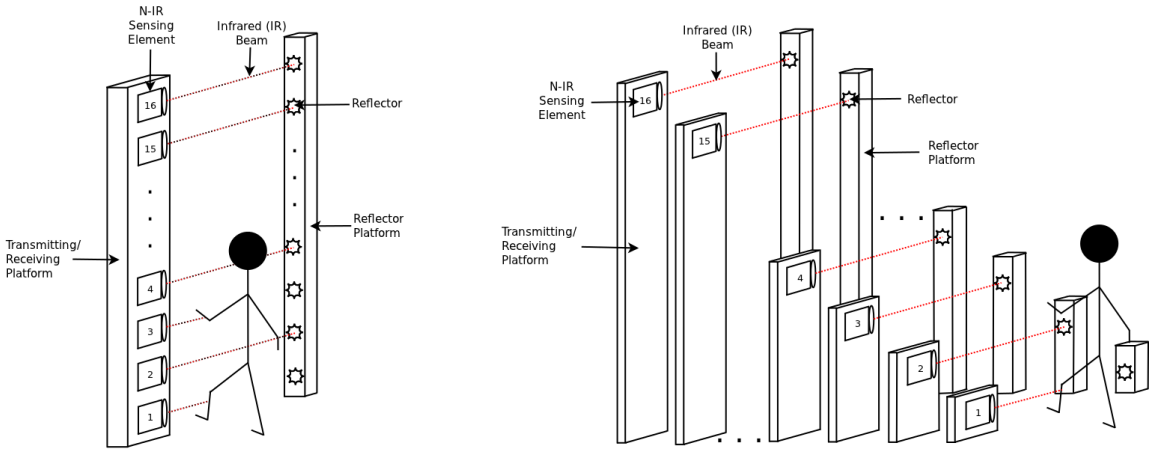

Fig. 2.1. Wired N-IR profiling sensor. (a) Sparse vertical array of detectors and (b) Sparse vertical array of detectors with custom horizontal offset.

The modifications in the second prototype not only supported horizontal offsets of the detectors, but also improved off-line data collection of the device. The second prototype employed the same sensing elements, transmitters, and reflecting surfaces as the original vertical array prototype but supported a modified detector configuration with horizontal offsets between sensing elements (Figure 2.1(b)) [17, 18]. Additional hardware improvements were made to eliminate the need of a computer in the field for data collection. An embedded microcontroller, Digi International BL4S200 single-board-computer, was utilized to illustrate that collecting, storing, realigning, and classifying data could be performed by a low-resource device. In addition, a hand-held interface I/O box, developed by Reynolds et al. [18], facilitated data access through a microcontroller by allowing view access of classification results in the field.

The sparse vertical detector array and the subsequent design with horizontally offset detectors provided a proof of concept that objects could be reliably classified by the silhouettes produced by these low-resource profiling sensors. A wireless version of such a sensor would improve deployment options and also facilitate the design of a network-centric profiling sensor environment. The third profiling sensor prototype focused on enhancing the horizontally offset version of the profiling sensor to a sustainable wireless model thereby increasing options for custom detector placement, which will increase deployment options in potential applications.

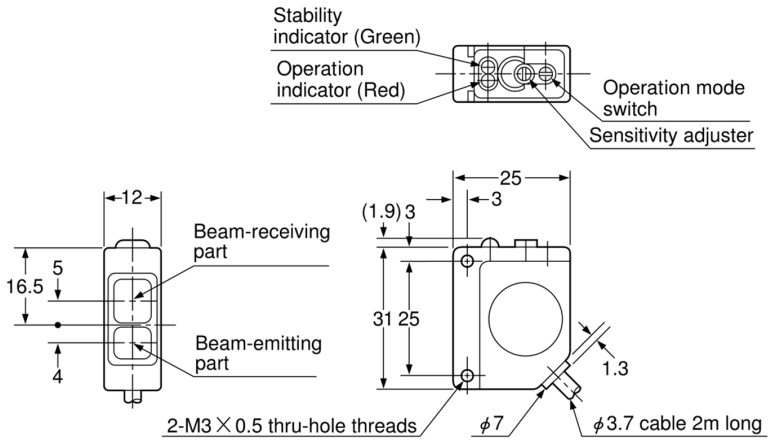

Fig. 2.2. CX-RVM5 retro-reflective photoelectric sensing element (all units mm) [19].

2.1.1 Sensing Element

The SUNX CX-RVM5 sensor (Figure 2.2) was chosen as the sensing element for the wired proof of concept prototype as it provided a robust sensing element adequate for our design needs [1, 5]. As the wired prototype was originally intended to be deployed in the desert of the southwestern United States, it was imperative that the components be able to tolerate a variety of temperatures and environmental conditions. This photoelectric sensor met all of these original requirements and produced

successful data capturing in both laboratory and field testing. The IP67 waterproof construction, with its resin-filled case, prevents water damage and protects against vibrations [19]. Moreover, it can withstand temperatures ranging from $-25\,^{\circ}\mathrm{C}$ to $60\,^{\circ}\mathrm{C}$ without loss of integrity. Its robust design allows for successful use, even in the extreme conditions of the deployment field.

In addition to an environmentally robust design, the SUNX CX-RVM5 sensing element must meet the functionality requirements of the wired profiling sensor. To complete a successful profiling sensor network, many of these small, concealable sensors must work in tandem at close range while maintaining a high recording frequency that captures enough feature details from all passing objects. The built-in interference protection function allows for close range mounting of these sensing elements within the profiling sensor without data loss or corruption. Despite the ability to mount the sensing elements at close range, the FOVs do not overlap because they are extremely narrow. Due to the $\sim$ 1kHz sampling rate, the profiling sensor is able to capture an image of a passing particle that only appears for 1ms within the 5m range. With the close placement of the sensing elements and the high sampling rate, it is nearly impossible for an object to pass undetected across the profiling sensor FOV, thus meeting the functionality requirements of the design.

2.1.2 Assembly

The earliest vertical array profiling sensor was composed of four main components: a transmitter pole, a receiver pole, a Universal Serial Bus-Digital Input/Output-32 (USB-DIO-32) interface box, and a power supply. Each pole was constructed from a $2' \times 4'$ studs that, when completed, stood over six feet tall (Figure 2.3). For the transmitter pole, 16 transmitters, manufactured by SUNX corporation, were mounted with 5" spacing between each sensing element. Likewise, 16 reflectors were mounted on a second pole with the same 5" spacing among reflectors. Although the components and materials provided a working, low-cost assembly, its size made this first design

difficult to transport [17]. Due to these difficulties, field deployment was impractical and thus, this design called for improvements.

These improvements were implemented in the vertical and custom array profiling sensors, which became significantly easier to transport and assemble in both field and lab environments. Chapter 2.1.2.1 will describe the assembly of one pair of sensing elements. Finally, Chapter 2.1.2.2 will discuss how the new design improvements were translated into the custom array profiling sensor.

Fig. 2.3. Prototype Sensor array constructed with 2'x4' studs [17].

2.1.2.1 Vertical Array Assembly

A second version of the vertical prototype was built using Polyvinyl Chloride (PVC) pipe segments, which allowed the vertical profiling sensor to be disassembled into smaller components for easier transportation, deployment, and storage. The PVC array was designed for decomposition into eight pieces, each containing two sensing elements [17]. An alternative PVC design was considered but eventually was discarded. The alternative design contained 16 segments per pole, with one sensing element for each segment. This led to a high number of electrical and physical

connections necessary to produce a complete assembly. By mounting two sensing elements per segment, the segment length remained approximately one foot and the profiling sensor required half as many connections as the single element segment design.

Based on this assembly configuration, eight identical stackable components, each containing a pair of N-IR detectors, made up the transmitter pole of the profiling sensor array. Two PVC T-couplings were used to mount one pair of detectors to the main frame of the profiling sensor. Each T-coupling was outfitted with two 3/4" adjustment holes for access to the sensing element sensitivity dimmer and its body for pairing alignment. One N-IR transmitter was mounted at the vertex of the T-coupling on an L bracket that was secured to the interior wall with two screws (Figure 2.4). The same process was repeated for a second T-coupling, which was then joined to the first through a segment of PVC pipe by leaving a 2" gap between the connectors (Figure 2.5). After mounting the sensing elements into the T-couplings and joining the couplings together, the wires from both N-IR transmitters were passed through the bottommost rear adjustment hole (Figure 2.6). Finally, the wires of the assembled sensing component were joined with a single port Category 6 (CAT6) keystone jack as shown in Figure 2.7. The resulting transmitter pole was assembled by stacking eight sensing components in a vertical arrangement.

Similar to the transmitter pole, the receiver pole was composed of eight PVC segments. These were made out of 2" diameter PVC pipe and were cut to the same approximate length as one completed transmitter segment on the transmitter pole. Two reflecting surfaces were mounted on each PVC segment with velcro, mirroring the spacing of the transmitter segments (Figure 2.8). The completed segments were then stacked vertically to construct the completed receiver pole of the profiling sensor. Finally, both the receiver pole and the transmitter pole were attached to a wood-constructed base for stability. The resulting profiling sensor, comprised of both transmitter and receiver poles, is shown in Figure 2.9.

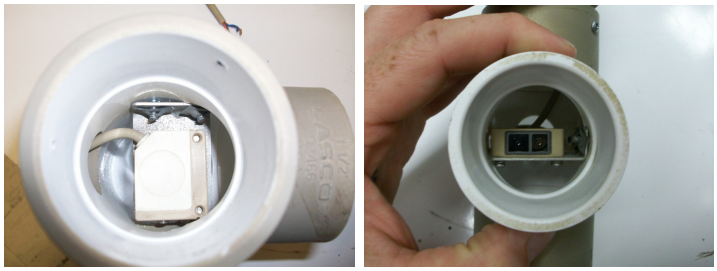

(a) (b)

Fig. 2.4. Mounting L bracket. (a) Top view of L bracket mounted inside PVC T-Coupling and (b) Front view of L bracket mounted inside PVC T-Coupling.

Fig. 2.5. A pair of joined T-couplings with sensing elements mounted inside.

The two other major components of the profiling sensor are the USB-DIO-32 interface box and a power supply. The USB-DIO-32 is a portable device that features plug and play, which allows for quick connections and disconnections to Universal Serial Bus (USB) 1.1 and 2.0 ports [20]. This digital Input/Output (I/O) product is optimized for applications without human interface, such as the profiling sensor. The Windows-based custom function driver maximizes data throughput capacity while the high speed USB bus allows for rapid transfer of data. Each of the 4 ports in the

USB-DIO-32 is an eight-bit digital I/O port capable of taking in data from 32 sensing elements. Considering the profiling sensor is currently made up of 16 sensing elements, only two ports, B and C, are in use. Since the output signals of one sensing element are continuous series of bits at $\sim$ 1kHz, the outputs of a single sensing element can be collected with a computer by channeling them through one of the multiple I/O pins in the USB-DIO-32.

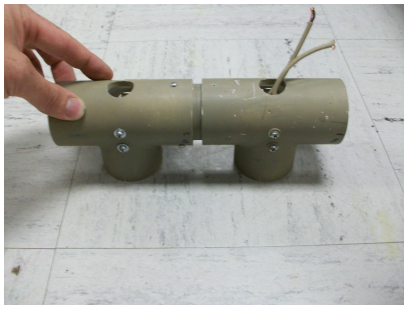

Fig. 2.6. Wires from both N-IR transmitters passed through the bottom-most rear adjustment hole.

The power supply was comprised of an array of resistors arranged into a voltage divider circuit, which supplied power to each of the 16 sensing elements in the profiling sensor. The pins of the two Data Bus-37 (DB-37) female connectors were assigned to provide power to, as well as data transfer from, the individual sensing elements of the profiling sensor to the USB-DIO-32 box via a fifty-pin Insulation-Displacement Connector (IDC) connector. The large fifty-pin IDC connector was the default input connector from the manufacturer, ACCESS I/O Product Inc., of which only 16 out of the 50 pins were in use.

Additionally, custom designed cabling was used to connect the power supply to the profiling sensor. The semi-octopus cable is a combination of standard connectors and cables that were combined to create a custom connector cable for use between the profiling sensor and the power supply. Since the sensing elements of the profiling sensor were connected by pairs into one Registered Jack-45 (RJ-45) female jack, only

8 ethernet cables were needed for connections. These standard ethernet cables were used merely as conducting media between the RJ-45 connectors and the power supply box. Two semi-octopus cables, with four ethernet cables each, were needed for full connection between the eight RJ-45 connectors of the profiling sensor and the power supply. Figure 2.10 shows an interface diagram of each of the components described thus far.

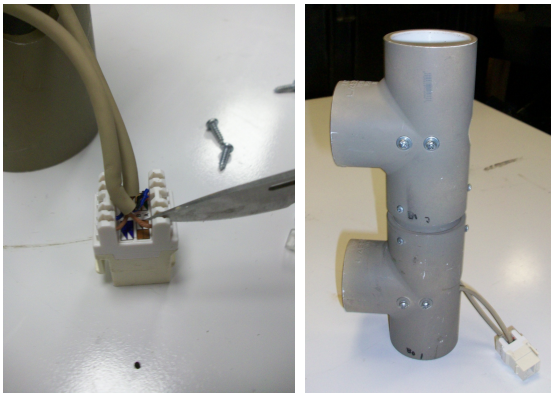

(a) (b)

Fig. 2.7. Assembled sensing components joined by a CAT6 jack. (a) CAT6 jack punching close view and (b) Assembled components of one sensing pair joined by a CAT6 keystone jack.

2.1.2.2 Custom Array Assembly

Since the configuration of the second prototype was segmental, it made for easy conversion to the custom horizontal offset array. No changes to equipment were necessary; however some software changes were needed. The only modification required for object classification using the horizontal array was within the algorithm used to compose the realigned silhouette. The necessary algorithm modifications will be discussed thoroughly in Chapter 2.1.3.

(a) (b)

Fig. 2.8. Receiver pole made up of 16 reflecting surfaces mounted with velcro. (a) Reflecting pole back view and (b) Reflecting pole front view.

Fig. 2.9. Finished vertical N-IR profiling sensor comprised of 16 elements making up the transmitter pole and an opposite pole with paring reflecting surfaces.

In addition to the software modifications needed in the data realignment of the custom array N-IR profiling sensor, supplementary hardware has been introduced to

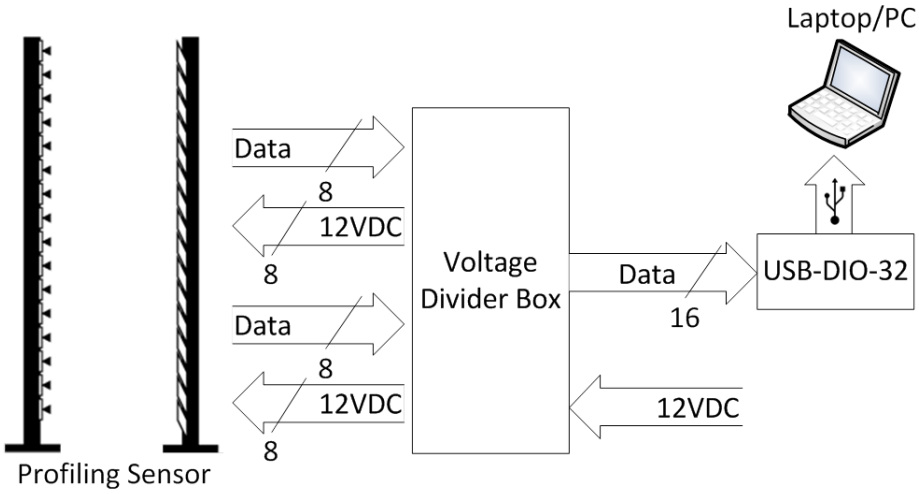

Fig. 2.10. Connection of components interfacing a profiling sensor with a lapto/PC.

make the system operate offline without the need of personal computers. Making the profiling sensor run autonomously is one of the objectives towards the goal of a ready-to-deploy system that can collect data without the need of a graphic user interface or other cumbersome hardware like a monitor, mouse, or keyboard [17]. Therefore a microcontroller has been used for this particular application to acquire, process, and classify data into predefined categories.

Fig. 2.11. Rabbit® 4000 Low-EMI, High-Performance Microprocessor [21].

The microcontroller of choice for this application is the Rabbit® 4000 Low-EMI, High-Performance Microprocessor [21] (Figure 2.11). This microcontroller can operate at a maximum clock speed of 60 Hz, store up to 1 MB of code, and support up to 16 MB of memory, sufficient for the purposes of this research [17]. The clock speed of this microcontroller allows for exceptionally fast logical and mathematical calculations necessary in the processing of binary data from the profiling sensor. Furthermore, this microcontroller can be programmed using Dynamic C®, a user-friendly programming environment that provides the programmer with the advantage of switching between C and assembly language while coding.

The Rabbit® SBC BL4S200 Series Single-Board Computer [22] (Figure 2.12) is a flexible platform that comes equipped with a Rabbit® 4000 microcontroller. This board is built to provide microprocessor control and I/O ports that can be used for timing events and reading equipment, such as the profiling sensor. Additionally, this board includes a mass storage support with the hot-swappable, industry standard miniSD™ memory cards that can be ejected from the board to be read in by other equipment, such as a laptop computer. Likewise, the BL4S200 board can be connected to a PC using a USB cable to debug code with the help of multiple features, including break points and watch expressions, among others, oriented toward real-time embedded systems programming.

Fig. 2.12. Digi® BL4S200 Single Board Computer [22].

The introduction of the Rabbit® board as part of the custom N-IR profiling sensor prototype, required adaptation of the power supply box. The additional DB-37 connectors were added to channel binary data coming from the profiling sensor to the input port of the Rabbit® board. These were added by simply splitting the input data pins so that both the USB-DIO-32 box and Rabbit® could receive the incoming binary data simultaneously. Figure 2.13 is a schematic of the profiling sensor's hardware connections including the new upgrades. This board was the first step towards making the wired N-IR profiling sensor a more autonomous system, but this design still leaves room for improvement in future generations of sparse array profiling sensors.

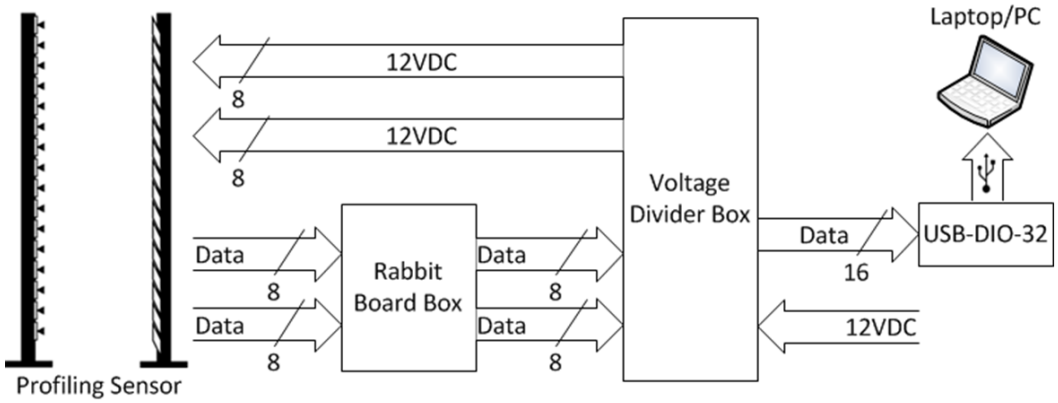

Fig. 2.13. Connection of components interfacing a profiling sensor with a BL4S200 single board computer [22] and a laptop/PC simultaneously.

In an effort to completely eliminate the need for a computer, to either operate the profiling sensor or to monitor classification results from collected data, a handheld I/O box (Figure 2.14) was developed to interface with the Rabbit® board. For convenience, the new handheld I/O box was built using the complementary hardware components from the Rabbit® development kit that included a collection of keypads and Liquid Crystal Display (LCD) devices. For the design advantage of the I/O box,

the largest LCD in this collection of components was selected and interfaced with a keypad in a separate box. With this handheld display, the classification results can be accessed and reviewed while the Rabbit® microcontroller box remains stationary, near the profiling sensor. By implementing this method, personnel monitoring the area can view classification results without cumbersome equipment; the only additional cabling needed between the I/O box and the microcontroller enclosure is a 6' Recommended Standard-232 (RS-232) cable and an Ethernet cable. The RJ-45 jack and its cable were used in this box to communicate between the I/O box and the Rabbit® board, which was chosen purely for its availability. This final piece of equipment, though auxiliary in capacity, greatly reduced the barriers to use currently seen.

Fig. 2.14. Handheld I/O box (bottom) interfaced with a with the Rabbit® board box (top).

2.1.3 Data Acquisition

The sixteen sensing elements in the profiling sensor are a set of parallel infrared beams that constantly take samples of its current state, broken or unbroken beam, at approximately 1kHz. An object walking across these beams would therefore, produce a series of "on" and "off" events, that for simplicity are recorded as a binary `1` and `0`, respectively (Figure 2.15). Since each sensing element records these events

according to a fixed sampling rate, the recorded data of a slow passing object would produce longer binary strings than for a passing object crossing the beams a faster speed [18, 23, 24]. For instance, a human walking across the profiling sensor would generally produce longer strings than a vehicle since the later is more likely move at a higher velocity. Therefore, the resulting raw data of one passing object can be represented as a $16 \times m$ binary matrix, where 16 is the number of sensing elements in the vertical sparse array, each row being the binary data of one sensing element. The number of columns in the binary matrix is left as variable n, because as just discussed, the length of the string depends upon the speed of the object crossing the specified trail. This binary matrix would eventually be used to generate a raw silhouette image of the object (Figure 2.16) and as input data for additional processing.

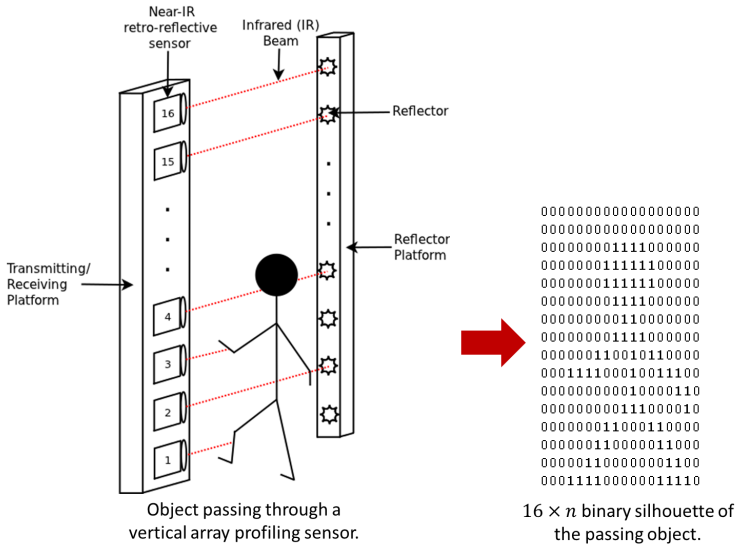

Fig. 2.15. Resulting binary matrix data from an object passing through the N-IR beams of a vertical array profiling sensor.

Moving forward with a more concealable version of the profiling sensor, a custom array profiling sensor with horizontal offsets between sensing elements was successfully implemented (Figure 2.17). The binary strings produced by this prototype resulted

in similar raw data as generated by the vertical prototype. Thus, the same concept regarding the speed of the object versus the string length also applied to the final $16 \times n$ binary matrix custom array profiling sensor.

Even though the horizontal offsets resulted in a more easily camouflaged device, it also introduced an offset distortion to the resulting binary data (Figure 2.18). Consider a vertical rectangle moving at constant velocity across the beams of the vertical N-IR profiling sensor. Intuitively, the binary silhouette generated by the vertical system should look as shown in Figure 2.19, given that there is no horizontal spacing between sensing elements in the profiling sensor. The lack of horizontal spacing between sensing elements makes it as simple as stacking the recorded samples one above the other to generate the silhouette image [18]. However, applying the same scenario to the custom array N-IR profiling sensor, a moving object takes more time to pass through the horizontal range of the custom array profiling sensor. This causes the system to record blank data (0's) from sensing elements where the infrared beam is unbroken while the object reaches the last sensing element in the array. As a product of this distorted data, the raw image is expressed with offsets relative to the horizontal distances between the sensing elements in the array (Figure 2.20). Since the lack of horizontal offsets did not occur in the vertical array, no further processing was necessary to correct a distortion.

With further processing necessary for the desired image production and classification, an algorithm was developed to correct for the horizontal offset caused in the data by the new configuration. The first step to remedy this issue is to perform a calibration. For this process a vertical rectangle, moving at an approximately constant speed, is passed straight across the custom array of detectors. By counting the samples between the initial trigger, when the leading edge of the rectangle breaks the beam of the first detector in the array, and the next trigger, the offset can be calculated and used to realign the data collected from the next detector in the array relative to the first [17,18]. Likewise, the same technique can be used once the leading straight edge reaches subsequent detectors to realign their corresponding data relative

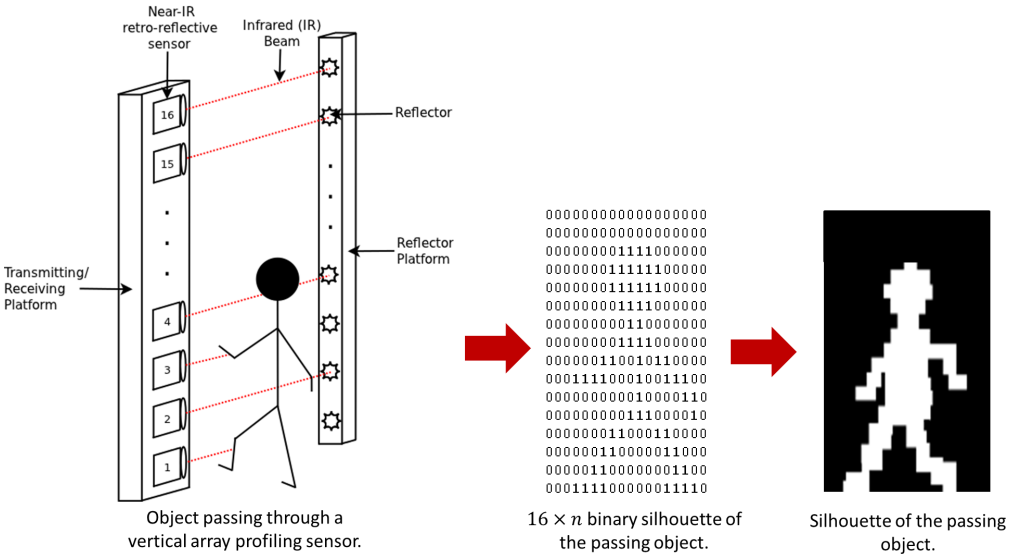

Fig. 2.16. Resulting binary data and silhouette from an object passing through the N-IR beams of a vertical array profiling sensor.

Fig. 2.17. Custom array profiling sensor with horizontal offsets between sensing elements [17].

to the first detector. Figure 2.21 shows how the silhouette of a traversing object can be realigned using this method.

Using the same technique to count the samples between each detector for data realignment, the velocity of a passing object can be approximated in cases where there

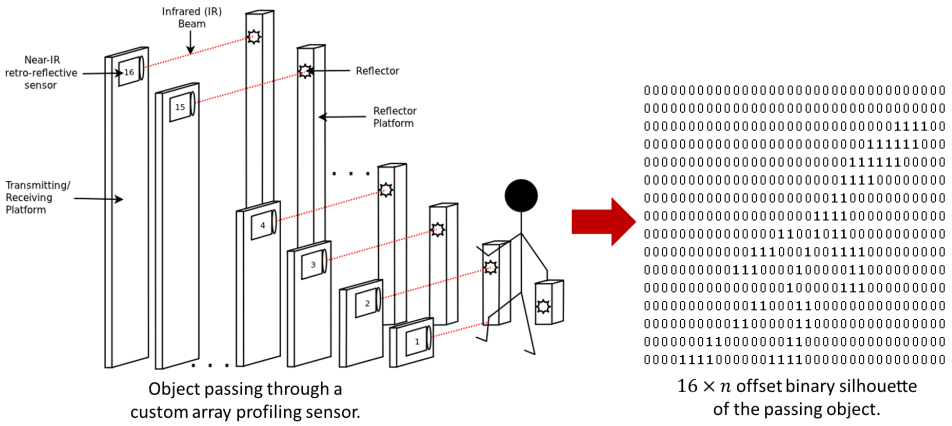

Fig. 2.18. Resulting binary matrix data from an object passing through the N-IR beams of a custom array profiling sensor.

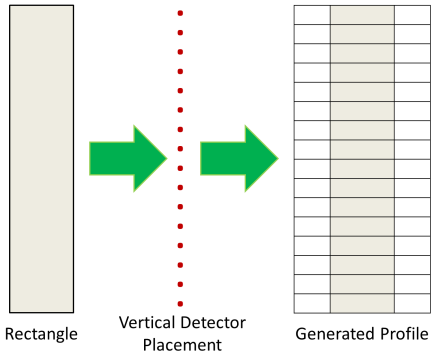

Fig. 2.19. Vertically straight rectangle passing through vertical array N-IR profiling sensor.

is a predetermined distance between the detectors [17]. To attain the average velocity of the object over the entire range of the sensor array, every inter-sensor velocity of the array must be calculated, not merely the velocity between adjacent sensing elements. The formula stated in Equation 2.1 expresses a two dimensional weighted average of the velocities across the entire array, where i and j are the initial and final sensing

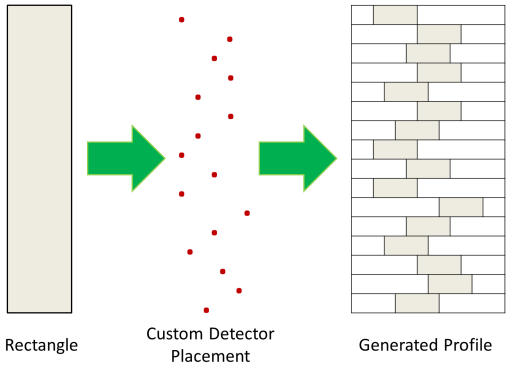

Fig. 2.20. Vertically straight rectangle passing through custom array N-IR profiling sensor.

elements of interest, respectively, v_{ij} is the velocity among elements calculated by Equation 2.2, and M is the number of sensing elements in the array [18, 24]. Notice that the velocity indicated by Equation 2.2 is calculated by dividing the distance over the time it took the passing object to move from sensing element i to sensing element j. This weighted velocity approach can also be used in silhouette realignment, but notice that in this case it is necessary to have at least an approximate measured distance.

Both methods of data realignment, either by calculating the average velocity of the object or by using a vertically straight rectangle, are not convenient realignment strategies if multiple profiling sensors are deployed in the field. The reason is that for the vertically straight rectangle the user would need to repeat the calibration with a rectangle passing at constant speed for each profiling sensor deployed in the field. Likewise, calculating the average velocity of the object across the sensor would require the user to manually measure and record the relative horizontal distance among sensing elements in each array. However, the latter realignment strategy would work better in situations where the relative distance between sensing elements could be calculated automatically, such as for wireless networks where this feature can be

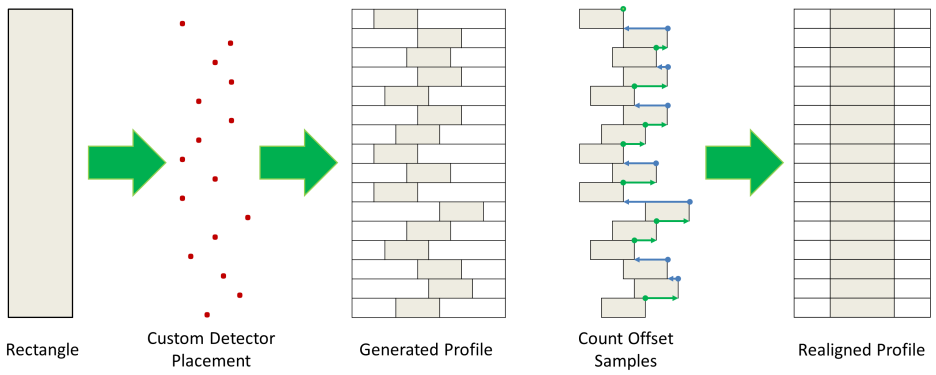

Fig. 2.21. Vertically straight rectangle passing through custom array N-IR profiling sensor before and after realignment algorithm.

supported. Even though both manual methods are better than having no realignment algorithm, these are cumbersome strategies that would make custom array profiling sensors harder synchronize and deploy.

$$\bar{v} = \frac{2}{M(M-1)} \sum_{i=1}^{M-1} \sum_{j=i+1}^{M} v_{ij} \tag{2.1}$$

$$v_{ij} = \frac{d_{ij}}{t_{ij}} \tag{2.2}$$

$$P_x = \sum_{i=1}^{8} \left(s_i \times 2^{i-1} \right) \tag{2.3}$$

In addition to the offset arrangement of the sensing elements in the second iteration of the profiling sensor, a low-resource microcontroller has been programmed to collect data without the need of a computer. As mentioned previously, the microcontroller of choice in this experiment is the Rabbit BS4S200 single-board-computer. This board has two 8-bit input ports, P_1 and P_2, which both can be combined to receive binary data from the 16 sensing elements in the N-IR profiling sensor. Port P_1 is used to record binary data from the lower half of the profiling sensor corresponding to 8

sensing elements, while P_2 is used to record binary data from the upper 8 sensing elements. To record the binary strings from the upper and lower sensing elements, Equation 2.3 is used to create $8 \times n$ binary matrices from both halves. Equation 2.3 is a one dimensional sum that creates an 8-bit string by reading the on-off value of the corresponding position, s_i, and shifting it to the appropriate position in the string, multiplying by powers of two. The microcontroller is capable of collecting data at a frequency up to 60 Hz, which is substantially lower than the sampling rate of the sensing elements that collect data at 1kHz. However, experimentation has shown that the lower sampling rate of the microcontroller is still sufficient to provide enough detail for accurate object classification or other processing [25].

3. WIRELESS PROFILING SENSOR

The wireless profiling sensor is the latest advancement in the category of N-IR profiling sensors and is the major contribution by the author of this work. The wireless profiling sensor is comprised of sixteen wireless N-IR sensing elements, each emitting an infrared (IR) beam across a designated trail (Figure 3.1). Compared to the prior work in N-IR profiling sensors, there are three major advances with this new sensor. First, the sensor is wireless and it sends data to a remote base station. Second, it uses an alternative technology for its sensing elements, that is, its detectors. With previous N-IR profiling sensors, a collection of transmitter and receiver pairs were required to detect an obstructing object along the path of an emitting IR beam. In the enhanced wireless prototype, a sensing node was configured to include a sensing element that does not require a mounted reflecting surface to detect a broken or unbroken beam event. The third significant improvement is in the data transmission method. Unlike the previous models where continuous streams of data were collected, the sensing nodes of the wireless prototype produce a bit of data corresponding to a broken or unbroken beam that is transmitted to the base station only when a state transition occurs. A few of the motivations to design wireless profiling sensor are:

- To produce a readily concealable device.
- To improve data collection efficiency.
- To improve power usage since battery consumption is a significant design constraint.

The third iteration of the profiling sensor discussed in this Chapter has been built with new hardware components to provide wireless features and increased power consumption efficiency. This wireless N-IR profiling sensor is not intended to provide

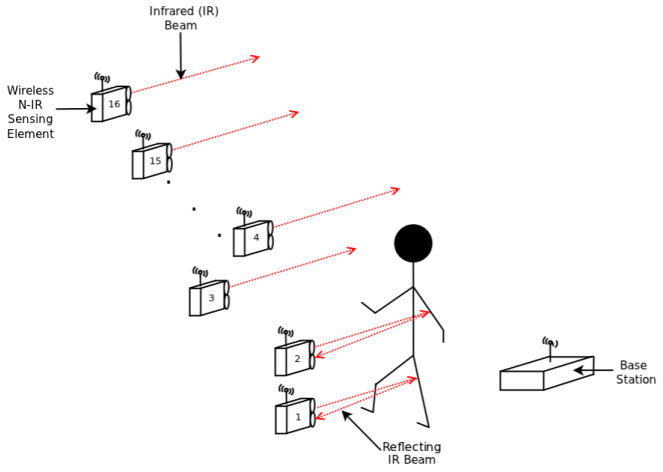

Fig. 3.1. Wireless N-IR profiling sensor with custom horizontal offsets.

a complete solution to the hardware and software limitations given in the first two prototypes. Instead, this third prototype is intended to be the first generation of wireless prototypes with a more battery efficient system. Additionally, similar concepts of data compression and generation, as used in previous iterations of the prototype, are implemented prior to classification.

The following chapters provide details about the hardware, assembly, and software developed for the wireless profiling sensor. Chapter 3.1 discusses the new sensing device used to realize the detectors. The assembly Chapter, 3.2, provides an overview of how the wireless N-IR profiling sensor was assembled. Next, Chapter 3.3 explains the data acquisition by the time segmentation method to generate the binary matrices used to generate silhouettes. Furthermore, to show the additional work involving the wireless N-IR profiling sensor, Chapter 3.4 and Chapter 3.5 will introduce the GUI application that processes incoming raw data and the classification of this data into three classes via a back-propagation neural network, respectively. Finally, Chapter 3.7 will discuss current deployment issues related to the current wireless prototype model.

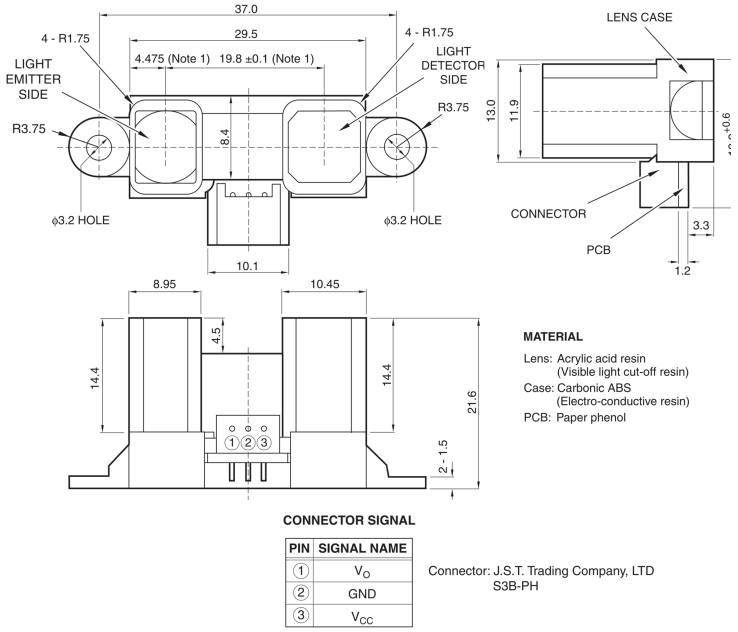

Fig. 3.2. Sharp GP2Y0D02YK0F distance measuring sensor with integrated signal processing and digital output [26].

3.1 Sensing Element

To make the wireless profiling sensor independent from a pairing reflective surface, the Sharp GP2Y0D02YK0F [26] (Figure 3.2), a N-IR distance sensing device, was used to detect objects along the path of each sensing element. The Sharp sensing element is a single point distance module, which measures the distance from the emitting infrared diode to the reflecting surface of the object. Furthermore, the effect of environmental light or the reflective properties of the sensed object on the GP2Y0D02YK0F is not significant up to a distance of approximately 80 cm. The N-IR distance sensor module utilizes the triangulation principle: the laser path is initiated at the N-IR beam emitter, reflects off of the object, and is captured by the imager. When this event occurs, the output line of the sensing element is set to a logical high; otherwise, it is set to low. The relationship between the emitter, object,

and imager is shown in Figure 3.3. The horizontal distance from the emitter to the object relies on the following: 1) the angle created between the emitted laser path to the object and the reflected laser path to the imager; and 2) the distance between the IR beam and the imager. The horizontal distance can be easily calculated by Equation 3.1, while Equation 3.2 utilizes the sine of the angle alpha to determine the horizontal distance [27].

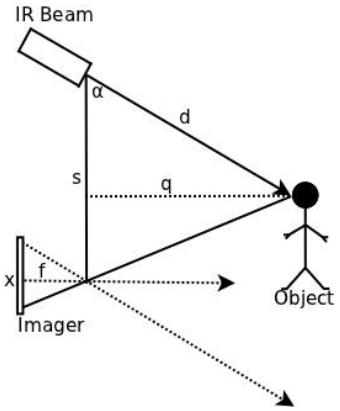

Fig. 3.3. Relative distances and angle between object and individual elements in the distance sensor.

$$q = \frac{(f)(s)}{x} \tag{3.1}$$

$$d = \frac{q}{\sin(\alpha)} \tag{3.2}$$

3.2 Assembly

The wireless profiling sensor prototype is made up of a collection of sixteen wireless sensing nodes. An example of one of the sensing nodes is shown in Figure 3.4(a). Each sensing node is constructed from a combination of off-the-shelf components, including the Sharp GP2Y0D02YK0F sensing element (Figure 3.4(b)). Additionally,

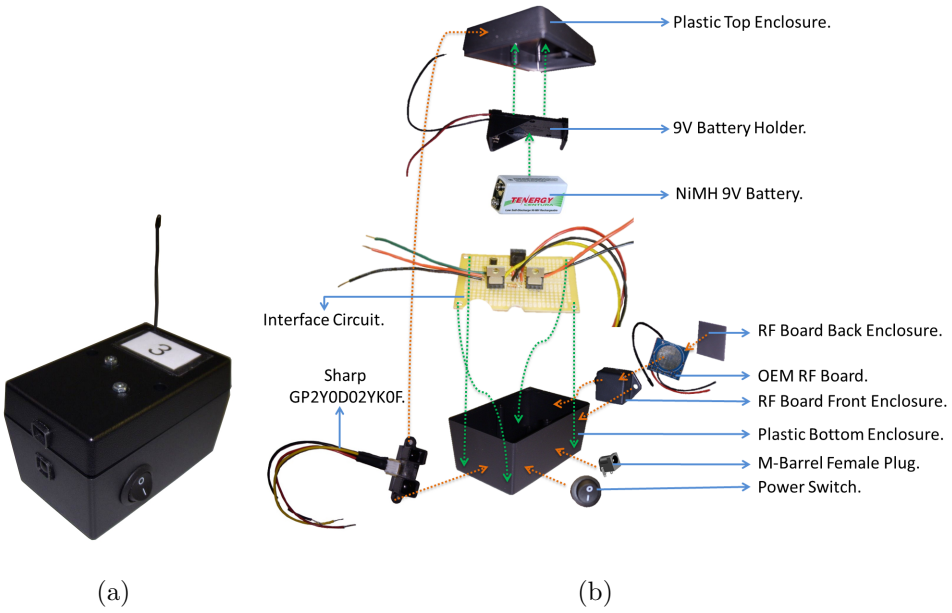

Fig. 3.4. Wireless sensing node. (a) Assembled view of one node and (b) Exploded view of one sensing node showing its internal components.

to make the sensing node wireless, each sensing element has been hardwired to its own wireless transmitter: an Original Equipment Manufacturer (OEM) Radio Frequency (RF) board [28] (Figure 3.5). Sixteen sensing nodes were used in the first wireless prototype to provide consistency with respect to prior N-IR profiling sensor designs and to facilitate comparisons to prior work. In practice, it is anticipated that the number of sensing nodes, that is detectors, would be determined by the required probability of identification and tolerable false-alarm rate permitted for the sensed object by the application of interest. All sensing nodes in the wireless profiling sensor communicate with a remote computing device, such as a Personal Computer (PC), via a USB gateway (Figure 3.6). The components shown in Figure 3.4 and 3.6 are necessary for the basic function of the wireless N-IR profiling sensor. The node charging station and related cabling are non-essential accessory devices, but they improve the ease of use of the wireless profiling sensor in laboratory development scenarios, as well as in field tests.

The signal regulator circuit divides the supply voltage to meet the specifications of the proximity sensor and wireless transmitter, using 5V and 3.3V of the original 9V, respectively. To increase the power stability due to a discharging battery, a series of voltage regulators were incorporated into the design. A switching Positive Negative Positive (NPN) transistor is used to close a circuit between the output of the proximity sensing element and the digital input of the wireless transmitter in order for the transmitter to detect when there is an infrared beam obstruction in the proximity sensor. In addition, a voltage regulator is placed in series with the base of the switching transistor to further regulate the digital output signal traveling from the proximity sensor to the transmitter. Figure 3.7 shows a schematic of this circuit design.

Fig. 3.5. OEM RF Board.

Since the profiling sensor is designed for deployment in a remote location, it was necessary to provide a power solution that would require little maintenance in a laboratory or field-test environment, albeit the sensor will be considered disposable for some anticipated applications. The power supply is a collection of off-the-shelf Nickel-Metal Hydride (NiMH) battery chargers, which resulted in a simplistic design, effectively eliminating the need for battery replacement. The focus during the design of this recharging station was on preservation of battery life. The charger includes a

Fig. 3.6. USB gateway receiver.

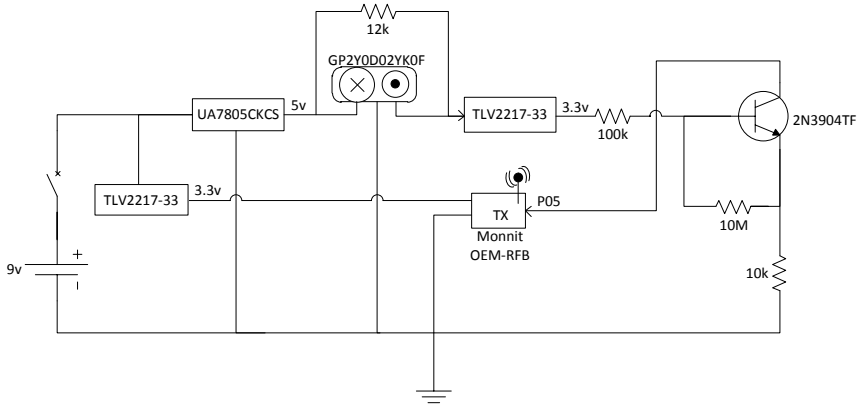

Fig. 3.7. Circuit schematic of the internal component configuration of one wireless sensing node.

microprocessor that automatically controls the charging process. With this control feature, all batteries within the 10 channels are able to maintain a full charge without overcharging and causing battery damage. By choosing a charging station that only contained the needed features, the cost remained low for the power supply. The power supply contains two of these 10 channel recharging stations. For this design, only 16 of the channels are in use as the profiling sensor only requires the use of one 9V battery per sensing node. The two recharging stations are housed in an Acrylonitrile Butadiene Styrene (ABS) box for protection from the elements. Wires

connect the output channels of the recharging station through an M-barrel connector for external access (Figure 3.8). The power supply draws power externally from one of two sources: the solar panel or a standard 60Hz, 120VAC wall outlet. The power supply uses whichever connected source provides the highest potential once the latter is converted to 12VDC. This power supply box makes the recharging process for the wireless profiling sensor batteries convenient and efficient since it minimizes personnel time and optimizes battery life.

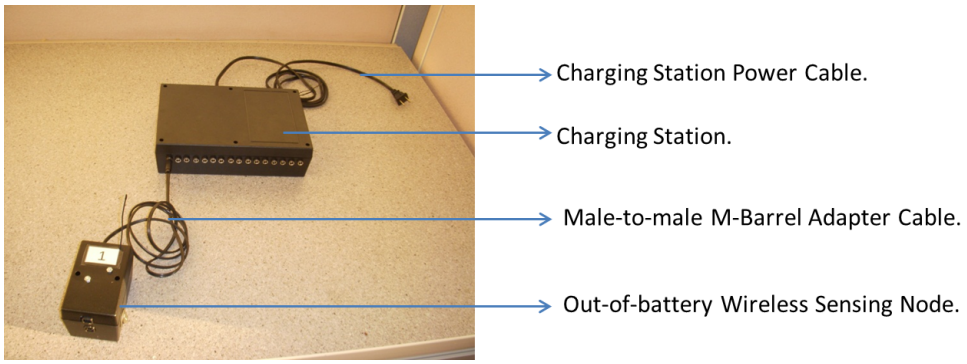

Fig. 3.8. One sensing node connected to one of the sixteen power outputs available.

3.3 Data Acquisition

To gain sufficient data to classify a passing object, the status of each node must only be known at two stages: when the object first obstructs the beam and when the beam is restored. Previous profiling sensor prototypes utilized a constant collection of data at a set frequency for its method of data acquisition [23, 24]. As previously mentioned in Chapter 3.2, a similar data acquisition method would quickly drain the battery of the wireless profiling sensor since the transmitter needs to pull current for every packet transmission. Therefore, we have implemented a data acquisition method that not only uses the battery more efficiently, but only uses one data packet

per change of state from each sensing element to generate the necessary raw data. With this method, the node is will not actively send data to the base station even if when it is constantly checking the state of the N-IR beam in each sampling cycle.

In the wireless profiling sensor, there is a designated trigger node that alerts the base station to the presence of an object. When this node detects an obstruction, the base station will begin recording data from all sensing nodes for a period of time specified in the sensor's configuration setup. A packet contains the state of the node and the source node identification number. The state of the node is a binary code in which zero (0) indicates an unbroken beam and one (1) indicates an obstructed beam. As the base station collects data packets from the various sensing nodes that comprise one wireless profiling sensor, it will also record the time in milliseconds of when each packet is received. After the specified recording time expires, the base station ceases to record data. The recording of one object during this period of time is denoted as one recorded event. The base station sorts the collected transmission records of the event by source node identification numbers. Then an algorithm determines the time length of the recorded event by calculating the difference between the time stamp of the final packet received and the time stamp of the initial packet received. In previous prototypes, time stamps were unnecessary because of the continuous data recording, but since this new prototype collects data only when a change of state occurs, we must generate the frequency of data acquisition for our non-constant rate to develop a binary matrix representation of this data.

The resulting binary matrix is a $16 \times m$ matrix in which every entry corresponds to a low or a high bit reading at a point in the sampling. To generate this matrix with the collection of time samples received, the total time length of the recording Δt is calculated by subtracting the time of the first packet received t_0 from the time the last packet is received, t_f. Equation 3.3 is then used to find the length of a time segment that will eventually be replaced by a binary value corresponding to the node state in that time interval. Additionally, $t_b - t_a$ is the time difference from a change of state within Δt. As shown in Equation 3.4, $t_b - t_a$ is divided by the result in Equation 3.3 so

that this time interval can be interpreted as a sequence of bits describing the constant state of the (t_a, t_b) interval. Figure 3.9 is a visual representation of this procedure. Repeating this procedure for each sensing node generates the 16 necessary binary rows making up the entire binary matrix. Finally, this matrix is used to generate a silhouette of the sensed object, as well as input data to a back-propagation neural network for subsequent object classification.

$$s = \frac{\Delta t}{256} \tag{3.3}$$

$$N = \frac{t_b - t_a}{s} \tag{3.4}$$

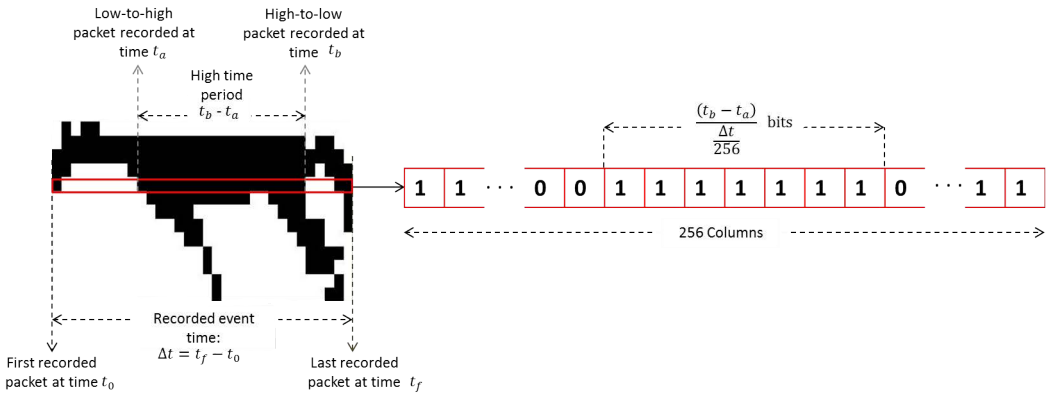

Fig. 3.9. Populating a binary row by using a time segmentation method.

3.4 Software Interface

Additional software was developed to support the development and test of the wireless version of the profiling sensor including the silhouette viewer and classifier. The software was divided into four different tabs, each providing a separate tool for the developer. The first tab, the silhouette viewer, displays silhouettes from

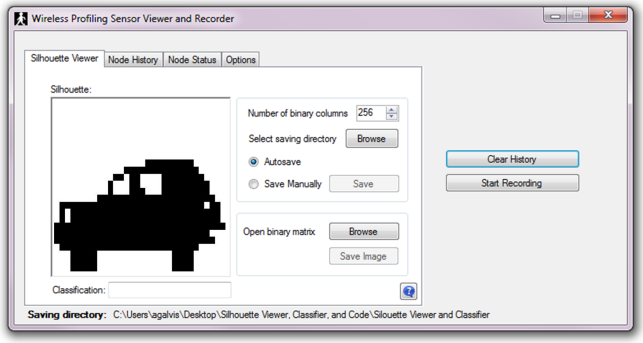

Fig. 3.10. Silhouette viewer tab.

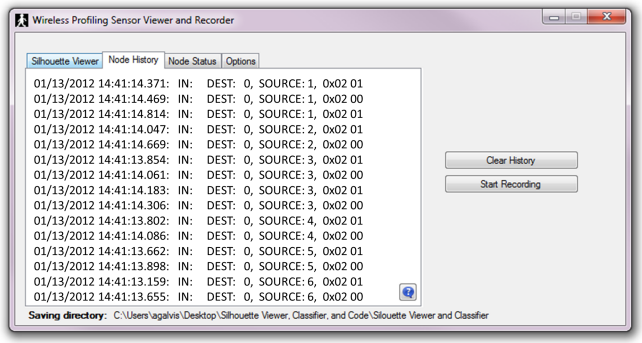

Fig. 3.11. Node history tab.

previously recorded binary matrices, or from data being currently collected. Figure 3.10 provides a screenshot of the "Silhouette Viewer" tab. The second tab is the node history tab, which displays a list of node ID's along with their current state (1-high, 0-low) at the time when each packet was received. Figure 3.11 shows a screenshot of the "Node History" tab. The third tab is the node status tab, which shows 16 icons corresponding to the current status of each sensing node. The status of each node can be one of three possible statuses: "No packet received", "IR-beam obstructed", or "IR-beam restored". Figure 3.12 shows the list of icons that represent the different statuses listed. Finally, the options tab (Figure 3.13) is divided into weights and

recording options. The weights option allows the user to choose from a preloaded weights file or a different file from a newly trained neural network. The recording option lists the different ways available to record new data from the wireless profiling sensor. The user may choose to stop recording after a time limit, have a trigger node that activates the recording of data for a time frame, or manually start and stop each recording event. Once the user begins record new data, the new recorded event is stored in the specified directory as three separate files:

- `Binary Matrix`: .txt containing the binary matrix of the recorded event.
- `Node Status`: .txt that stores a sorted version of what is displayed in the "Node History" tab. This node history is sorted by node ID.
- `Silhouette`: .bmp that displays the silhouette of the recorded event.

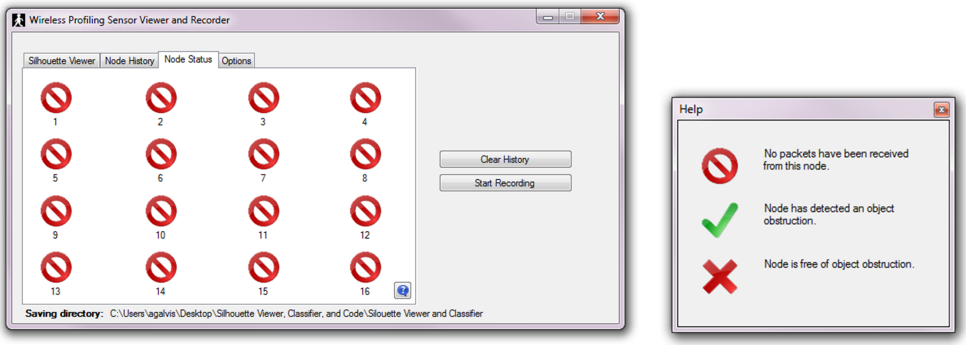

(a) (b)

Fig. 3.12. Node status. (a) Node status tab and (b) Node status display icons.

3.5 Classification Algorithm

The purpose of the classification algorithm is to accurately classify the data acquired from the wireless profiling sensor into predefined classes, for example, classify

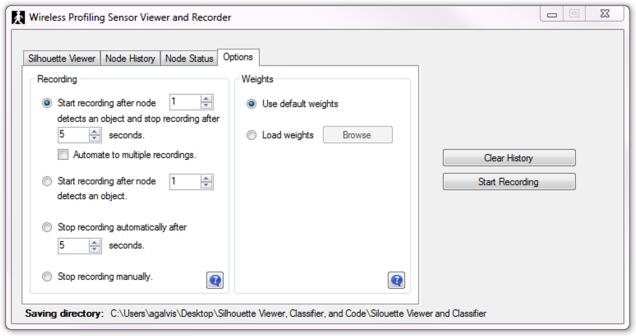

Fig. 3.13. Options tab.

the data as human, animal, or vehicle. Classification is achieved through the use of a three-layer back-propagation neural network. The outputs of the neural network classifies data into one of the three predefined classes of objects. Chapter 3.5.1 discusses the data processing algorithm that adjusts the size of data to the same number of inputs in the back-propagation neural network. For completeness, some neural network fundamentals are summarized in Chapter 3.5.2 before the network configuration and results are shown in Chapter 3.6.

3.5.1 Preprocessing of Existing Data Library

As discussed in Chapter 3.5, a back-propagation neural network was trained and tested with a defined number of human, animal, and vehicle samples. However, the original raw data included samples with varying column sizes due to variations in the passing object's velocity, the sensing element's sampling frequency, and the horizontal spacing between sensing elements. Since a back-propagation neural network requires a predefined number of inputs, the number of columns in each sample of the preexisting library have been compressed using an algorithm that fixes the number of binary columns to a predefined dimension. Recall that one binary row in the matrix represents the recorded binary sequences of one sensing element, thus for sixteen sensing

elements in the N-IR sparse array profiling sensor, sixteen rows will be generated to build a complete matrix. However, for the various reasons listed above, the number of sensing elements in the sparse array cannot predict the number of columns in the output matrix. Therefore, this chapter will describe the algorithm implemented to compress a binary matrix to a fixed number of columns.

Because of the $\sim 1kHz$ sampling rate of the vertical profiling sensor, the vast majority of the original data was generated with over one thousand columns. Previous work by Reynolds et al. [25] shows that most of the characteristic features of a silhouette are not noticeably affected upon visual inspection when a matrix is significantly compressed. To show proof of this concept, a collection of samples with over one thousand columns was compressed to 16×256 binary matrices to observe if major visual differences between the original and compressed data exist. Figure 3.14 shows three silhouettes from a human, animal and vehicle before and after compression. Notice that the only feature loses were of small pixels, whereas the integrity of the characteristic features remained intact.

To begin the column compression process, consider a binary matrix with an original dimension size of $16 \times n$. Let c be the number of desired resulting number of columns after compression, and for simplicity, assume that c divides n into a natural number d (i.e. $S = \{nd \mid nd = c;\ c,\ n \in \mathcal{N},\ n \leq c \wedge c|n\}$). A window of size d slides over binary substrings of the same size until covering the entire length of one row before continuing to the next. As the window encloses the current d-bit binary substring, the number of zeroes and ones are counted to calculate the bit value that occurs most often within the window. Finally, all bits in the window are removed and replaced by one bit; the most common bit value in the window. However, by default, if d is an even number and there are exactly $\frac{d}{2}$ ones and $\frac{d}{2}$ zeros, the window is replaced by a bit value of one. After the d-bit binary substring is replaced by its most common bit within the window, the window slides to the next d-bit substring. This process is repeated until reaching the end of the binary matrix.

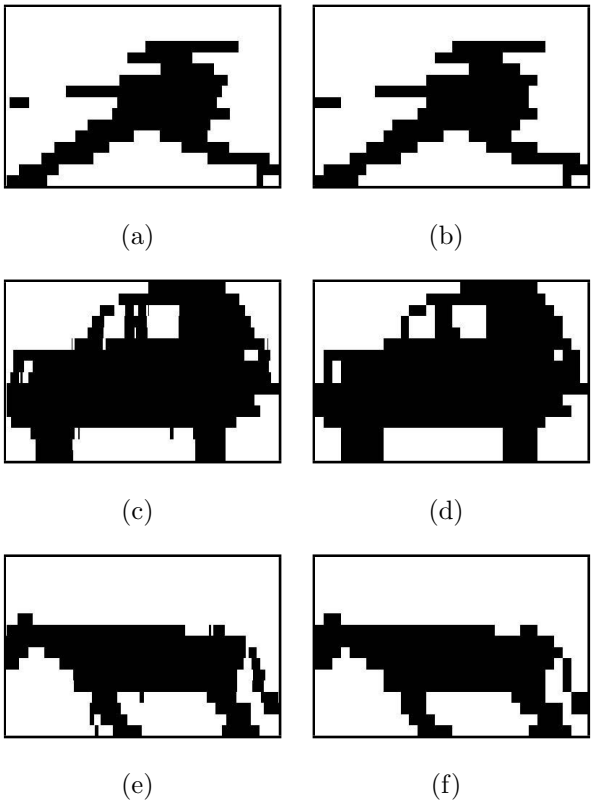

Fig. 3.14. Silhouettes before compression and after compression. (a) Human silhouette before compression, (b) Human silhouette after compression, (c) Vehicle silhouette before compression, (d) Vehicle silhouette after compression, (e) Animal silhouette before compression, and (f) Animal silhouette after compression.

A special case occurs when $c > n$, when the desired output matrix has more columns than the input matrix. Although an input matrix of this form does not occur often, the matrix preprocessing algorithm expands the number of columns to a predefined length. To begin this process, the number of original columns n are counted to divide c. Since n does not necessarily divide c, a remainder $r \geq 0$ must exist. Now consider an original input matrix that has $n = \frac{c-3}{2} \; \forall \; c > n$ columns, that is, the desired output matrix has twice as many columns as the original input matrix plus three additional columns. This means that the output matrix must be doubled and add $r = 3$ number of columns to it in order to adjust its size. To obtain

the desired number of columns in this example, every bit in the original matrix is replaced by two equal bits, then the remaining three bits are added by replacing three bits in evenly spaced positions by two bits of the same value as shown in Figure 3.15.

This chapter presents a solution by hardcoding a compression (or expansion) algorithm of binary matrix dimensions. However, other approaches may be implemented according to the programmers preferences as long as the end result of the modified matrices does not considerably alter the characteristic features of the silhouettes. That being said, the shape of a human silhouette should look similar in shape as its original counterpart in order to maintain consistent and comparable data between input and output binary matrices.

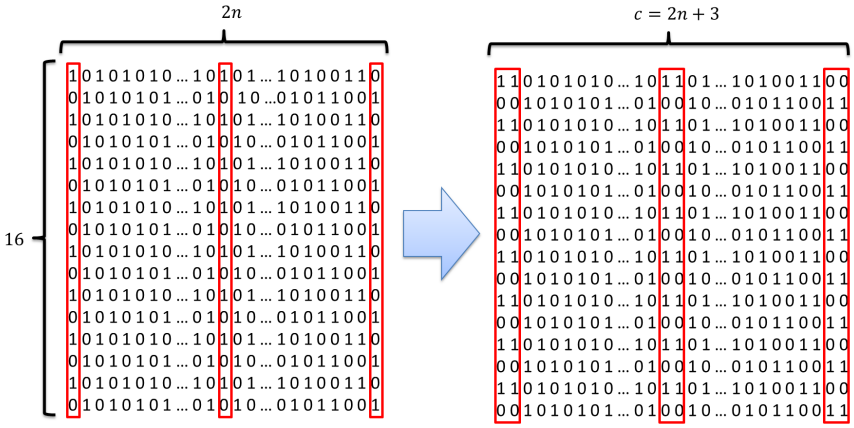

Fig. 3.15. Bit replacement in evenly spaced positions.

3.5.2 Neural Network

A neural network can be thought as system capable of processing a series of inputs in vector form to produce one output vector. Additionally, a neural network is a collection of weighted connections and processing elements in which the weighted connections pass values from the processing elements in the previous layer to the

next. A neural network can have multiple layers and different types of feeding patterns between processing elements. However, depending on the application, the more involved neural network topologies may be more difficult to train or may take more computational resources to process an input vector. Therefore, for simplicity, a three layer back-propagation neural network (with feedforward pattern matching) has been used here as this produces an output corresponding to the closest estimation for the given input. Finally, a few definitions concerning neural network key elements and concepts are presented below as summarized from Eberhart and Shi. [29]:

- `Network weights`: regulates the amount of dataflow passing from one processing element to the next. Weight connections can be excitatory if its value is positive or inhibitory if it is negative. A weight with value of zero simulates an absence of connection between the processing elements.

- `Processing elements`: neural network components where calculations are executed. A processing element can have single or multiple inputs that are passed down from other processing elements trough the network weights. Each processing element collects these local inputs to produce a single local output value. Additionally, these outputs can be the input to other processing elements or the output to the neural network.

- `Processing element activation function`: maps the domain of a processing element to a specified range. There are infinitely many functions that can be used to perform this mapping; however, functions that bound the output to a fixed range are often desirable because these often reduce computation time during training. A common activation function of choice is the sigmoid function as it has a bounded range for any real argument.

Although the original raw data had varying column dimensions [18, 23, 24], when using a library of over 1000 silhouettes captured in the field [30], including humans, animals, and vehicles, it has been shown that compressed data with a fixed number

of columns produces virtually no alterations in the silhouette resolution [25]. Since a back-propagation neural network is used to classify the data, a fixed number of inputs were required to obtain a classification result. After normalizing the data to 256 columns, the back-propagation neural network was trained with half the data set within the compressed library. This neural network is comprised of $256 \times 16 = 4096$ processing elements in the input layer, 20 processing elements in the hidden layer, and 3 processing elements in the output layer. This configuration was observed to provide the best classification results compared with other back-propagation neural networks with differing numbers of processing elements within the hidden layer. The method used to train the neural network was from Ebehart and Shi [29].

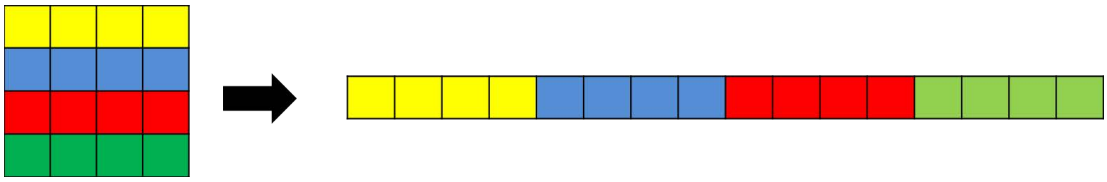

Fig. 3.16. Matrix vectorization: all rows from a two-dimensional matrix are put sequentially into a linear array.

To make the matrix easier to process by the neural network the binary matrix has been vectorized by sequentially combining all rows (Figure 3.16). Each processing element in the input layer uses each bit entry in the vector matrix as the argument to a sigmoid function (Equation 3.5), which will generate a real value between 0 and 1. The output values from each processing element in the previous layer become the input values for each of the processing elements in the subsequent layer. The edges connecting the processing elements from one layer to its subsequent layer have a weight value which is generated during the training process of the neural network. The weight of the edge is then multiplied by the input for each processing element in the hidden layer. The sum of these 4096 products becomes the argument for the sigmoid function of the hidden layer. This process is repeated from the hidden layer to

the output layer to generate three output values. A schematic of this neural network is shown in Figure 3.17. Equations 3.6 and 3.7 are used to calculate the input values to the processing elements in the hidden and output layer. The values v_{ih} and w_{ji} denote the weight values from the input to the hidden layer and from the hidden to the output layer, respectively, all which are generated during the training of the neural network. Furthermore, notice that the sum of products begin from $h = 0$ and $i = 0$, the bias processing elements, which take an input value of 1.

$$f(x) = \frac{1}{1 + e^{-x}} \tag{3.5}$$

$$y_{ki} = f\left(\sum_{h=0}^{n} \left((x_{kh})\,(v_{ih})\right)\right) \tag{3.6}$$

$$z_{ki} = f\left(\sum_{i=0}^{h} \left((y_{ki})\,(w_{ji})\right)\right) \tag{3.7}$$

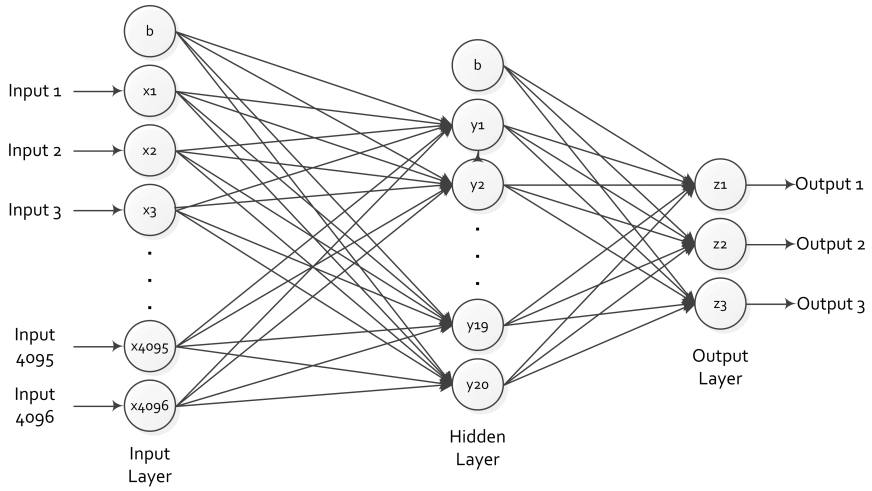

Fig. 3.17. Back-propagation neural network with 4096 input processing elements, 20 hidden processing elements, and 3 output processing elements. Bias processing elements are denoted by b and these take an input value of 1.

3.6 Results

Prior work with the first generation, sparse vertical detector array N-IR profiling sensors included a significant effort to build a comprehensive library of sensed objects, including numerous vehicles (e.g., motorcycles, cars, trucks, SUVs, ATVs, etc.), humans (e.g., men and women of various sizes and gaits, and carrying various loads, including backpacks and weapons), and animals (e.g., dogs, horses, llamas, etc., including carrying various loads) [30]. A back-propagation neural network to classify objects sensed by the wireless version of the profiling sensor was trained with approximately 580 samples from the comprehensive pre-existing library. An additional 577 samples from the pre-existing library was used to test the accuracy of the newly trained neural network. The number of human, animal, and vehicle samples used in both training and testing of the back-propagation neural network are shown in Table 3.1. Having a pre-existing data library of animals, humans, and vehicles expedited the training and testing of the neural network to be used in the new wireless sensor. A very small library of sensed human silhouettes acquired directly from the new wireless N-IR profiling sensor was also used to test the performance of the neural network trained with the pre-existing library. These results from data acquired directly from the wireless sensor are briefly summarized after the results when using the pre-existing library.

Table 3.1
Number of samples per class used in the neural network training and testing processes.

	Training	**Testing**
Human	337	333
Animal	81	81
Vehicle	162	163

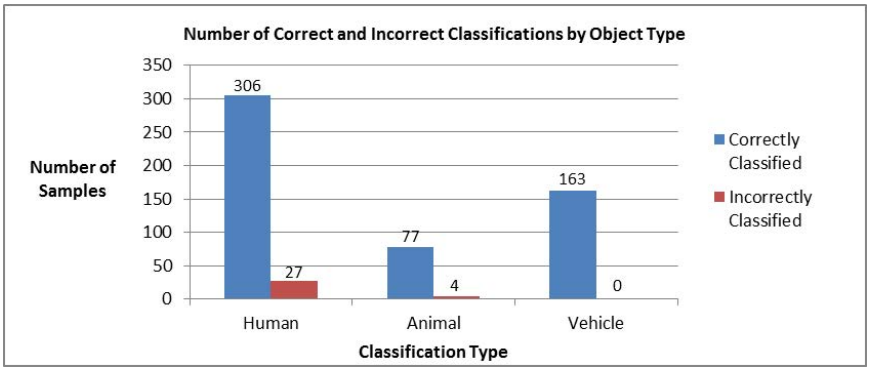

Fig. 3.18. Distribution of number of samples per class within the testing data set.

The neural network takes the binary values in the input layer to determine the result, shown in the output layer as positive real numbers between 0 and 1; the output processing element with the highest value indicates the classification of the input. Each test data sample was fed through the input layer of the neural network. The sequence of linear operations and activation functions used by each processing element are discussed in Chapter 3.5.2. These values are passed from one layer to the next until reaching the output layer, which indicates the processing element with the highest value and corresponds to a given classification (i.e., human, animal, or vehicle). The distribution of correctly and incorrectly classified test samples from each class analyzed is shown in Figure 3.18. The neural network classified 577 samples from the pre-existing library with 94% accuracy (Figure 3.20). A confusion matrix that shows the performance of the classification algorithm in this test is shown in Table 3.2. Finally, the tables of confusion for the human, animal, and vehicle classes are shown in Tables 3.3, 3.4, and 3.5 and the false positive rates per class are presented in Figure 3.19.

Recall, the classification results summarized in Figure 3.20 are when using the library generated by the first N-IR profiling sensor and not data acquired by the improved wireless profiling sensor. Building a comprehensive library with the wireless

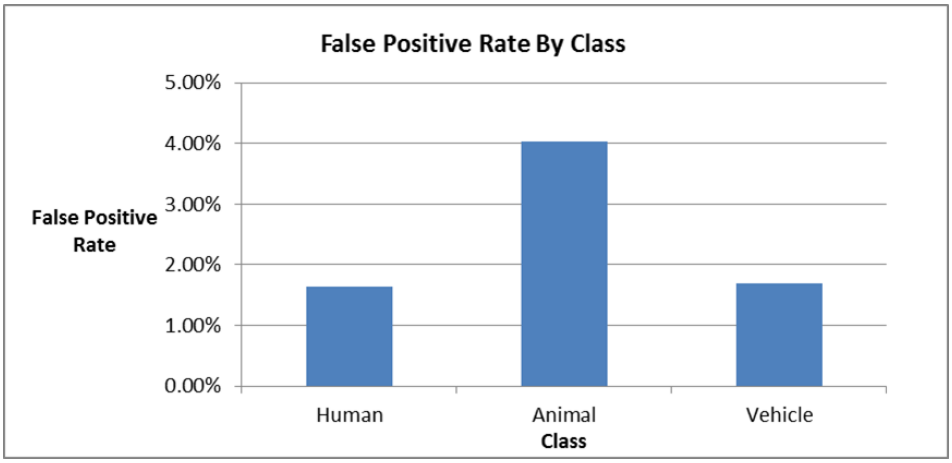

Fig. 3.19. False positive rate by class.

profiling sensor is future work and out of the scope of this thesis. Nevertheless, the new wireless profiling sensor was used to collect and classify 164 humans with 95.7% accuracy (with 7 objects incorrectly classified as animal). This preliminary data acquired directly from the wireless sensor has comparable accuracy to when using the original library. It is important to point out that constructing an object's binary silhouette by the time segmentation method in Chapter 3.3 requires receiving two change-of-state packets. Therefore, to prevent packet collision resulting in data loss, the wireless prototype detectors were arranged with small horizontal offsets of approximately 5-10 inches prior to data collection. Decreasing the horizontal offsets would likely increase the accuracy of the classification above 94% given that the neural network was trained with a pre-existing library from sensors with no horizontal offsets.

Therefore, for new configurations of the wireless N-IR profiling sensors detectors, where significant horizontal offsets are anticipated, it would be necessary to retrain the neural network with data collected from the new detector configurations, that is, from the new placements of the sensor nodes that comprise the overall wireless profiling sensor. Rapidly training the neural network given a wide-variety of sensor node placements, including ad hoc placements, is of very high interest and the subject

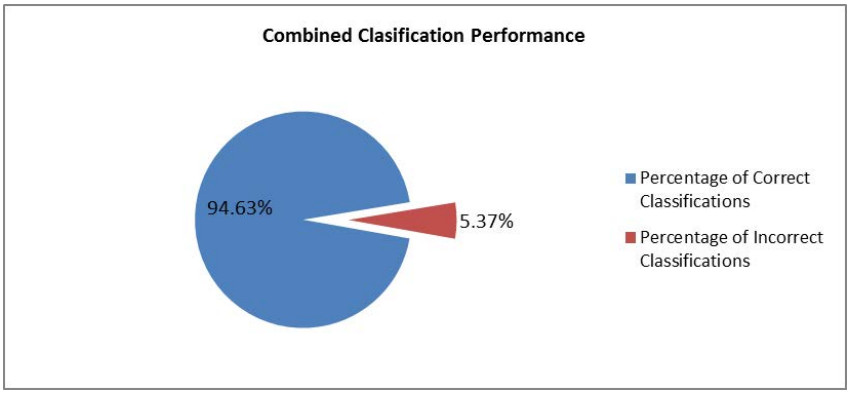

(a)

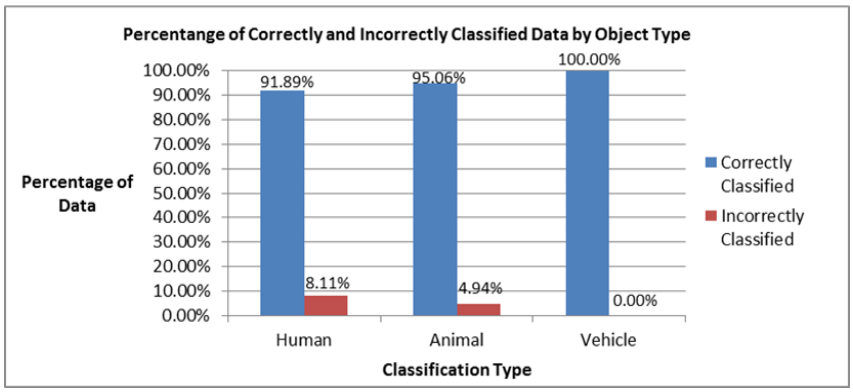

(b)

Fig. 3.20. Classification results. (a) Overall combined percent of correct and incorrect classification results and (b) Correct and incorrect classification results by object classes.

of future work. A current limitation of the existing wireless sensor design, including the neural network used for object classification, is that passing objects of the same type must have an approximately constant velocity. When a passing object changes its velocity in the horizontal space between each sensing node, the silhouette may become significantly distorted and classification results can be affected, unless a new neural network is trained to accommodate the variability of the velocity for objects of the same type.

Table 3.2
Confusion matrix of classification results.

		Predicted Class		
		Human	Animal	Vehicle
Actual Class	Human	306	20	7
	Animal	4	77	0
	Vehicle	0	0	163

Table 3.3
Table of confusion for the human class.

306 True Positives: Actual humans that were correctly classified as humans.	**27 False Negatives:** Humans that were incorrectly classified as animals or vehicles.
4 False Positives: Animals that were incorrectly classified as humans.	**240 True Negatives:** All remaining objects, correctly classified as non-humans.

Table 3.4
Table of confusion for the animal class.

77 True Positives: Actual animals that were correctly classified as animals.	**4 False Negatives:** Animals that were incorrectly classified as humans or vehicles.
20 False Positives: Humans that were incorrectly classified as animals.	**476 True Negatives:** All remaining objects, classified as non-animals.

Table 3.5
Table of confusion for the vehicle class.

163 True Positives: Actual vehicles that were correctly classified as vehicles.	**0 False Negatives:** Vehicles that were incorrectly classified as animals or humans.
7 False Positives: Humans that were incorrectly classified as vehicles.	**407 True Negatives:** All remaining objects, classified as non-vehicles.

3.7 Deployment Issues

Having a well concealed profiling sensor will improve its effectiveness as a security device since activities of interest are less likely to occur in known surveillance areas. Concealment is a deployment challenge for profiling sensors. The wireless prototype provides a proof of concept profiling sensor and it will enable more sophisticated options for concealment in real-world application scenarios.

There are many barriers to satisfactory concealment in the Southwestern United States. The natural features of the targeted area provides some advantage for concealment; however, most of the natural flora consists of short, thin-branched shrubs. Additionally, there are some elevated areas with rocky outcroppings and crevices, which would provide some cover to the device. Since natural features alone cannot provide adequate concealment, the device must be designed to be hard to detect, due either to its small size or its painted camouflaged cover.

Concealment has been one of the main design features that each iteration of the prototype has worked to improve in the profiling sensor. The first iteration provided the prototype that was the hardest to conceal. The sensors were attached to a 6' pole and wired to the base station. These large shapes do not often occur naturally in the desert, proving difficult to conceal. The second prototype, with the custom horizontal offset, provided a more natural shape for concealment despite the wired connection. The wireless prototype allows for similar placement and shape as the second prototype while eliminating the need for the wired base station. This prototype can more easily be concealed in a small cluster of bushes or in a rock outcropping than either of its predecessors.

Constraining an extensive region such as the Southwestern United States into a smaller area could increase the number of successful readings of human intruders in this area. Using a series of seemingly natural attractors and detractors would allow for funneling of the traffic crossing the border into smaller trafficking regions. For example, an artificially made lake in the desert would very likely attract subjects,

while placing some form of vegetation to block entry to some regions. By directing suspects into designated trails with surveillance equipment, the detection of such intruders would be more easily facilitated. The concept of using landscape for preventive and surveillance measures have been used in criminal justice studies since at least the early 90's [31]. Combining multiple strategies to conceal and deploy equipment in a larger areas may increase the success rate of detecting crime these areas; therefore, landscaping can help reduced the amount of equipment needed to cover an area, as well as give authorities a better estimate of where intruders are more likely to travel.

Improving the battery life of wireless equipment is particularly important for profiling sensors, as these sensors will be considered as disposable in many anticipated applications. The time segmentation method was used to reduce the amount of data sent from the sensor nodes to the base station, thereby reducing power usage, and increasing battery life. However, this process can be further optimized for minimal battery consumption. For instance, the sensing nodes could collect data at a specified sampling rate and then send the binary string collected from each height to the wireless base station for its further processing. In addition, the sensing nodes could communicate with each other once, immediately following deployment, such that all nodes that comprise a given profiling sensor would have recorded their relative position. Such a dynamic scheme will be particularly important for ad hoc distribution of sensor nodes. These positions could be used as additional information to realign the collected data and improve classification accuracy. These additional features would make up a more efficient, robust, and easier to deploy profiling sensor.

3.8 Limitations

Although there have been many design improvements in this third iteration of the sparse array profiling sensor, some limitations still exist. The first and unavoidable limitation is that the sensing elements cannot collect data when the object is in between nodes. This is why the assumption is made that the object is traveling

at an approximately constant velocity. If the passing object were to accelerate or decelerate greatly in the space of the horizontal offset, the realignment processes would be unable to account for the acceleration and the resulting silhouette would be distorted. Additionally, velocity of the passing object must remain below a sampling threshold. If the object travels across the sensing element at a velocity greater than that of the sampling threshold, the object will obstruct the beam only at a time when the sensing element is not sampling data. For example, the threshold for a human was calculated to be just over 70 miles per hour. Based on the timing chart in Figure 3.21 of the Sharp GP2Y0D02YK0F, there is an approximately 7ms gap between data captures. Using 250mm as the minimum width of a passing human, the speed necessary to bypass a sensing element undetected was 73.6 miles per hour. Although this velocity is unattainable for a human, this sampling threshold could come into play if a desired class of object traveled at an extremely high velocity.

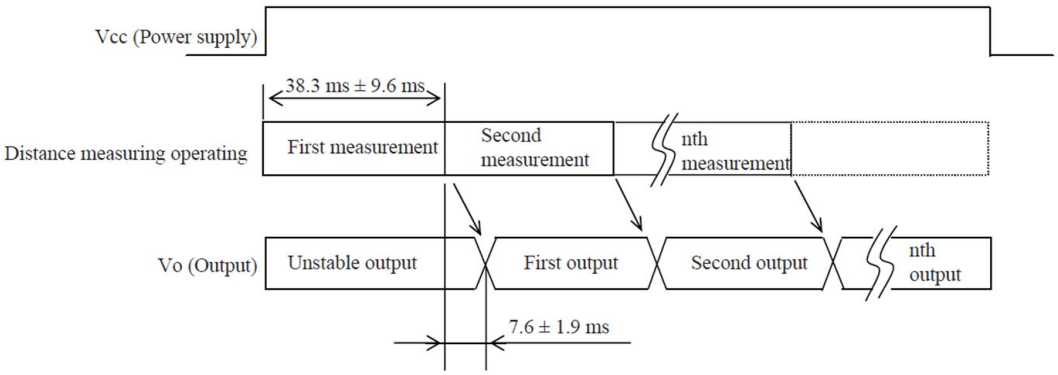

Fig. 3.21. Sharp GP2Y0D02YK0F timing chart [26].

Other limitations of the wireless device have arisen with the new data acquisition method. First, when data collision occurs, this prevents the data from being received at the base station. The missing data alters the silhouette and, depending on the amount and location of the missing data, this may cause to incorrectly classify a passing object. Future work includes modifying the network topology to address this

issue. The final limitation of note is the current inability to dynamically calculate the relative distance of nodes in the sparse array. This inhibits the deployment of the device as the current classification system requires the neural network to be trained on each node configuration before use.

4. ALTERNATIVE PROFILING SENSOR MODELS

In addition to the work performed on N-IR profiling sensors, alternative profiling sensor models are currently being pursued by other researchers to classify silhouettes, including a pyroelectric sensor and a 360° sensor. Both of these devices have the capability to support some of the same potential applications as the N-IR profiling sensors; however, at this time, such alternative approaches appear to be significantly more expensive than the sparse detector array profiling sensors previously discussed in Chapter 2. These alternative approaches typically forgo the sparse detector array for a more traditional dense focal-plane array and emulate a sparse detector array by extracting a subset of pixels of interest.

4.1 Linear Pyroelectric Array Profiling Sensor

The linear pyroelectric array profiling sensor is a passive system that uses long wave infrared (LWIR) detectors [9, 12, 24]. Unlike any of the N-IR profiling sensors described in Chapter 2, the pyroelectric approach does not generate radiation. Consequently, the pyroelectric sensor takes advantage of the radiation, namely heat, emitted by the objects of interest to generate a silhouette of the object in the camera's field of view. Such techniques typically use a denser focal-plane array as compared to N-IR profiling sensors and extract a subset of pixels of interest, in effect emulating a sparse detector array. With the pyroelectric approach, a four paneled blackbody was used to calibrate the infrared camera by determining the linear relationship between the preset temperatures and grayscale values. The collection of data, in the form of two-dimensional images, required techniques to achieve image segmentation, feature extraction, and classification results according to the system specifications.

The features of interest were first isolated and later defined through image processing. Since the background in the field of view remains stationary, it is eliminated from the image using velocity thresholding. A similar thresholding technique is used to convert the grayscale image to a binary black and white image. Figure 4.1 shows a block diagram of the profile generation process leading to the binary image used for classification from a passive IR sensor that emulates a profiling sensor by extracting a single column of detectors [9].

Several classification algorithms including a Naïve Bayesian, Naïve Bayesian with Linear Discriminant Analysis for dimensionality reduction, K-Nearest Neighbor, and Support Vector Machines were compared to study their performance classifying human and animals [9]. Brown et al. [24] use a Naïve Bayesian classification method that operates over "reasonably complete" binary images. The selected images under this category are binary images that contain sufficient features that can be used to easily identify the object in the image as a human or animal by the naked eye. Examples of these features are the head and arms of a human, which make the object in the image easily identifiable as a human. The same approach would apply for an animal for assignment into the animal classification. This method is highly successful at classifying passing objects, both in the laboratory and in the field as shown by Brown et al. [24], Chari et al. [9], and White et al. [12].

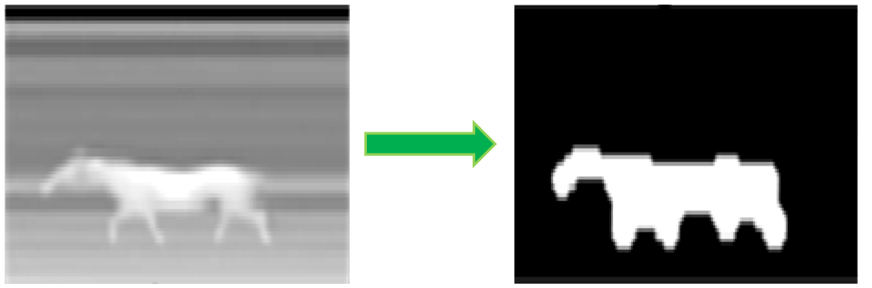

Fig. 4.1. Block diagram showing the process of simulation [9].

4.2 360° Profiling Sensor

The 360° profiling sensor is a non-sparse detector that uses a long wave infrared camera focused on a conical mirror to achieve a 360° field of view [32]. The conic mirror provides continuous field of view coverage in the horizontal regions but its size and shape constrains coverage in the vertical direction, though the cones are interchangeable. Since the maximum height of a target can be estimated and the design of the conic mirror can be changed to accommodate such vertical heights, full vertical coverage is unnecessary for anticipated applications.

$$\alpha = 90^\circ - 2\phi \tag{4.1}$$

$$\beta = 2\phi - 90^\circ + \frac{FOV_m}{2} \tag{4.2}$$

$$\phi = \arctan\left(\frac{h_c}{r_b}\right) \tag{4.3}$$

Figure 4.2 shows how the projection angles α and β can be calculated by using Equations 4.1 and 4.2, where FOV_m is the minimum field of view of the camera covered by the concentric conic mirror [32]. Equation 4.3 computes the internal angle of the cone base, ϕ, where h_c and r_b are the height of the cone and the radius of the base of the cone, respectively. Theoretically, these equations can be used to design a conic mirror to cover a new field of view, this being narrower or wider depending on the application of interest. However, different designs may distort the image further, thus making the segmentation, feature extraction, and classification algorithms less successful. Figure 4.3 shows the 360° profiling sensor model designed and built in the laboratory [32].

With this conical mirror, some image processing is necessary due to the radial distortion caused by the curvature of the mirror. Although the radial aspect of the image is distorted, the vertical image remains undistorted. For an object present

in the field of view of the 360° profiling sensor, several sample frames are taken and statistical analysis is used to separate the targeted object from its background. Brown et al. [32] explain the different statistical methods used to separate the image into the segment of interest in addition to feature extraction and classification methods.

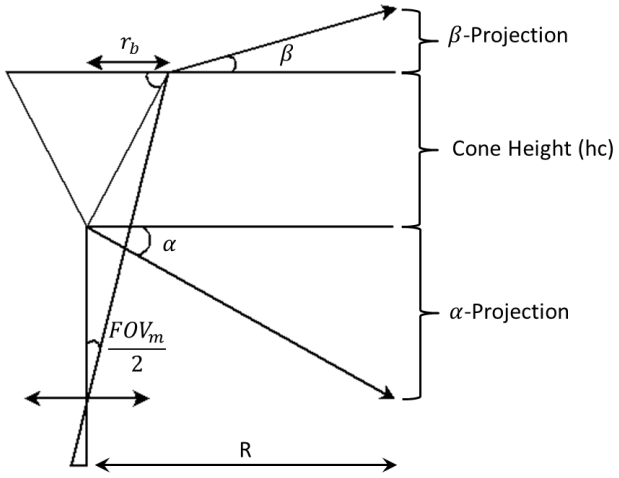

Fig. 4.2. Layout of a 360° profiling sensor [32].

Fig. 4.3. 360° profiling sensor prototype designed and built in the laboratory at the University of Memphis [32].

5. CONCLUSION

As shown by the results presented here and those in related articles, sensors that classify a crude silhouette are a reliable means of surveillance, especially for broad-scale object identification into classes such as human, animal, or vehicle. Several iterations of profiling sensors were developed and are still under development, including N-IR, pyroelectric, and 360° profiling sensors. Though each type of sensor operates differently to obtain the initial silhouette or profile, they all can function as a form of profiling sensor. The N-IR sensors, which utilize a sparse detector array, have evolved more rapidly than alternative approaches and appear to be a lower-cost option, which will be critical in application scenarios in which the sensors must be regarded as disposable. The iterations of N-IR profiling sensors have enhanced their design from a proof-of-concept vertical wired sensor array requiring a computer in-field for data acquisition to a customizable wired detector array with a microcontroller. This thesis advances that work to a customizable, sparse detector array realized as a collection of wireless sensor nodes whose data can be aggregated at a base station to realize a profiling sensor.

By combining the Sharp GP2Y0D02YK0F with an OEM RF board, a wireless profiling sensor prototype was designed and tested with highly accurate results in classifying passing objects at close range. As shown in these experiments, the Sharp GP2Y0D02YK0F proximity sensor can be used to collect data in a similar way to the CX-RVM5 IR based profiling sensor. The data collected by the proximity sensors is generated by using only two packets of data, one for a broken beam and one when the beam is restored. There is no significant loss of silhouette resolution when the normalized binary matrix is generated. Furthermore, this input into the back-propagation neural network is used to train and classify data, producing correct classifications with up to 94% accuracy. In addition to the increasing processing capabilities, the

flexibility to deploy these sensors in the field is increased by allowing each sensing node to have a horizontal offset. Overall, this new design of the profiling sensor is an incremental improvement as compared to the original, wired profiling sensor prototype.

Most significantly, the N-IR approaches, especially the wireless profiling sensor described in this thesis, have provided the most novel contribution toward profiling sensors, that is, sensors that can be remotely and randomly deployed in network-centric sensing environments for intelligent fence type applications. For example, N-IR profiling sensors have been used in data-to-decision ontology-based proof of concept frameworks, as well as in sensor fusion schemes [33,34]. Also, profiling sensors have been used in a conceptual framework for detecting human intent from external stimuli [35].

Although advances have been made in profiling sensors toward a more easily deployable, concealable, and energy efficient design, additional enhancements of the wireless prototype will be necessary before it is ready for practical deployment, including improvement packaging of the sensor node to withstand anticipated environmental conditions of the deployment site. Moreover, sensor-node to sensor-node communication to dynamically determine the relative locations of each node will enhance ad hoc deployment and training of the back-propagation neural network.

Future work will include continuing the improvements to the deployment and concealment of this device in a network centric type of environment. First, the wireless profiling sensor will be used to amass new data library from field tests.

Following determining the accuracy of the device in the field, the random deployment configuration feature will be developed so that the nodes will be able to automatically detect the relative location of the other nodes. This may reduce the need for training the neural network after deployment and convert the wireless profiling sensor to a dynamically adjustable system. To further improve deployment capabilities, work will be done to reduce or eliminate the collision of data transmitted to

the base station by improving the topology of the network and the communication between the profiling sensor sensing nodes and the base station.

Future work towards concealment include increasing sensing range and reducing node size. Other off-the-shelf components will be considered as well as in house manufacturing of component pieces to achieve these concealment improvements. Once the random deployment feature is in place, testing will be conducted to determine how increased horizontal offsets affect the classification accuracy of the improved wireless profiling sensor.

LIST OF REFERENCES

LIST OF REFERENCES

[1] D. J. Russomanno, S. Chari, and C. Halford, "Sparse detector imaging sensor with two-class silhouette classification," *Sensors*, vol. 8, no. 12, pp. 7996–8015, 2008.

[2] D. Russomanno, S. Chari, E. Jacobs, and C. Halford, "Near-IR sparse detector sensor for intelligent electronic fence applications," *Sensors Journal, IEEE*, vol. 10, pp. 1106 –1107, June 2010.

[3] R. B. Sartain, "Profiling sensor for ISR applications," vol. 6963, p. 69630Q, SPIE, 2008.

[4] J. Karl K. Klett, R. B. Sartain, T. Alexander, and K. Aliberti, "Optical and radiometry analysis for a passive infrared sparse sensor detection system," vol. 6941, p. 69410I, SPIE, 2008.

[5] D. J. Russomanno, M. Yeasin, E. Jacobs, M. Smith, and S. Sorower, "Sparse detector sensor: Profiling experiments for broad-scale classification," *Unattended Ground, Sea, and Air Sensor Technologies and Applications X*, vol. 6963, p. 69630M, April 2008.

[6] W. P. Dizard III, "DHS unveils massive, fast-track border project." Government Computer News, January 2006.

[7] C. Strohm, "Border tech program is plagued by early setbacks." Government Executive, June 2007.

[8] E. Jacobs, D. J. Russomanno, and C. Halford, "Profiling sensors for border and perimeter security," *SPIE Newsroom*, August 2009.

[9] S. Chari, C. Halford, E. Jacobs, F. Smith, J. Brown, and D. Russomanno, "Classification of humans and animals using an infrared profiling sensor," vol. 7333, p. 733310, SPIE, 2009.

[10] R. B. Sartain, K. Aliberti, T. Alexander, and D. Chiu, "Long-wave infrared profile feature extractor (pfx) sensor," vol. 7333, p. 733311, SPIE, 2009.

[11] S. Chari, F. Smith, C. Halford, E. Jacobs, and J. Brooks, "Range and velocity independent classification of humans and animals using a profiling sensor," vol. 7694, p. 76941K, SPIE, 2010.

[12] W. E. White III, J. B. Brown, S. Chari, and E. L. Jacobs, "Real-time assessment of a linear pyroelectric sensor array for object classication," vol. 7834, p. 783403, SPIE, 2010.

[13] K. Emmanuel, D. Russomanno, E. Jacobs, S. Chari, and J. Brown, "Silhouette data acquisition for a sparse detector sensor," SENSIAC, 2009.

[14] A. Galvis, D. J. Russomanno, and C. R. Kothari, "A wireless near-ir retro-reflective profiling sensor," vol. 8389, p. 83890R, SPIE, 2012.

[15] A. Galvis and D. J. Russomanno, "Advancing profiling sensors with a wireless approach," *Sensors*, vol. 12, no. 12, pp. 16144–16167, 2012.

[16] Z. Sun, P. Wang, M. C. Vuran, M. Al-Rodhaan, A. Al-Dhelaan, and I. F. Akyildiz, "Bordersense: Border patrol through advanced wireless sensor networks," *Ad Hoc Networks*, pp. 468–477, 2011.

[17] R. K. Reynolds, *Real-Time Object Classification Using a Custom Sparse Array Profile Sensor on an Embedded Microcontroller*. May 2011.

[18] R. K. Reynolds, S. Chari, and D. J. Russomanno, "Embedded real-time classifier for profiling sensors and custom detector configuration," vol. 8047, p. 80470E, SPIE, 2011.

[19] Anon, "CX-RVM5/D100/ND300R data sheet," 2007. Ramco Innovations.

[20] Access I/O Products Inc., "USB-DIO-32 32-channel digital I/O module data sheet," 2012.

[21] Digi International Incorporated, "Rabbit 4000 low-EMI high performance microprocessor," 2010. Sheet No. 91001568 B1/1210.

[22] Digi International Incorporated, "Rabbit SBC BL4S200 series single board computer," 2011. Sheet No. 91001510 B2/411.

[23] M. Yeasin, D. J. Russomanno, M. S. Sorower, M. Smith, and J. S. Shaik, "Robust classification of objects using a sparse detector sensor," in *IC-AI*, pp. 742–748, 2008.

[24] J. B. Brown, S. Chari, J. Hutchison, J. Gabonia, and E. Jacobs, "Assessment of a linear pyroelectric array sensor for profile classification," vol. 7693, p. 76930O, SPIE, 2010.

[25] R. K. Reynolds, D. J. Russomanno, S. K. Chari, and C. E. Halford, "Profiling sensor classification algorithm implementation on an embedded controller," vol. 7694, p. 769413, SPIE, 2010.

[26] Sharp Corporation, "GP2Y0D02YK0F distance measuring sensor unit," December 2006. Sheet No. E4-A00501EN.

[27] K. Konolige, J. Augenbraun, N. Donaldson, C. Fiebig, and P. Shah, "A low-cost laser distance sensor," in *Robotics and Automation, 2008. ICRA 2008. IEEE International Conference on*, pp. 3002 –3008, May 2008.

[28] Monnit Corporation, "Monnit WIT wireless temperature sensor," 2012. Sheet No. MD-001-1A.

[29] R. Eberhart and Y. Shi, *Computational Intelligence: Concepts To Implementations*. Burlington: Morgan Kaufmann, August 2007.

[30] D. J. Russomanno, S. Chari, K. Emmanuel, E. Jacobs, and C. Halford, "Testing and evaluation of profiling sensors for perimeter security," *The ITEA Journal of Test and Evaluation*, vol. 31, no. 1, pp. 121–130, 2010.

[31] T. Crowe, *Crime Prevention Through Environmental Design.* Butterworth-Heinemann, 2 ed., July 1991. ISBN-10: 0750690585.

[32] J. B. Brown, S. K. Chari, and E. L. Jacobs, "An assessment of a 360-degree profiling sensor for object classification," vol. 8047, p. 80470F, SPIE, 2011.

[33] C. Kothari, J. Qualls, and D. Russomanno, "An ontology-based data fusion framework for profiling sensors," in *Electro/Information Technology (EIT), 2012 IEEE International Conference on*, pp. 1 –6, May 2012.

[34] J. Qualls, D. J. Russomanno, and V. Bollu, "Integration of a profiling sensor onto sensor fabric," in *IKE'10*, pp. 250–254, 2010.

[35] C. R. Kothari, D. J. Russomanno, R. B. Sartain, and R. Frankel, "Toward data-to-decision sensing environments to assess human intent from responses to stimuli," *Ground/Air Multisensor Interoperability, Integration, and Networking for Persistent ISR III*, vol. 8389, pp. 838904–838904–8, May 2012.

APPENDIX

APPENDIX: N-IR WIRELESS PROFILING SENSOR HARDWARE AND SOFTWARE DOCUMENTATION

A CD-ROM containing the wireless N-IR profiling sensor's source code, related documentation, drivers, and software has been provided to the Indiana University-Purdue University Indianapolis (IUPUI) Purdue School of Engineering and Technology. Table A.1 lists the Monnit RF core board's related software and documentation in separate categories. Likewise, Table A.2 lists the N-IR wireless profiling sensor's software and documentation separated by different directories. For convience, all of these folders have been compiled into the same CD-ROM.

Table A.1
List of Monnit RF core board's related software and documentation with their descriptions and locations.

File/Folder	**Description**
IAR Embedded Workbench	Compiler used to edit and compile the OEM Monnit RF core boards.
Monnit Documentation	Documentation describing specific software functions run within the OEM Monnit RF core boards. Hardware specifications of the I/O the RF core board is also provided.
Monnit Gateway Drivers	Software drivers for the Monnit USB gateway for 32-bit and 64-bit Windows operating systems.
Monnit OEM Firmware	Monnit RF core board software files that control the RF board hardware such as I/O pins and packet transmissions.
SmartRF Studio Software Manifest	Software used to upload resulting *.hex files generated after compiling Monnit OEM Firmware files in IAR Embedded Workbench.

Table A.2
List of N-IR Wireless Profiling Sensor related software and documentation with their descriptions and locations.

File/Folder	**Description**
Profiling Sensor Data	Folder containing original data library from the vertical N-IR profiling sensor.
Profiling Sensor Data (Scaled at 256 Columns)	Folder containing compress data library from the vertical N-IR profiling sensor into a fixed number of 256 columns.
Back Propagation Neural Network	Back-propagation neural network C files.
Silhouette Viewer and Classifier (Source)	C# source code of the silhouette viewer and classifier.
Silhouette Viewer and Classifier	Executable version of the silhouette viewer and classifier.
SHARP GP2Y0D02YK Distance sensor.pdf	Documentation regarding the sensing element used in the individuals wireless N-IR sensing nodes.